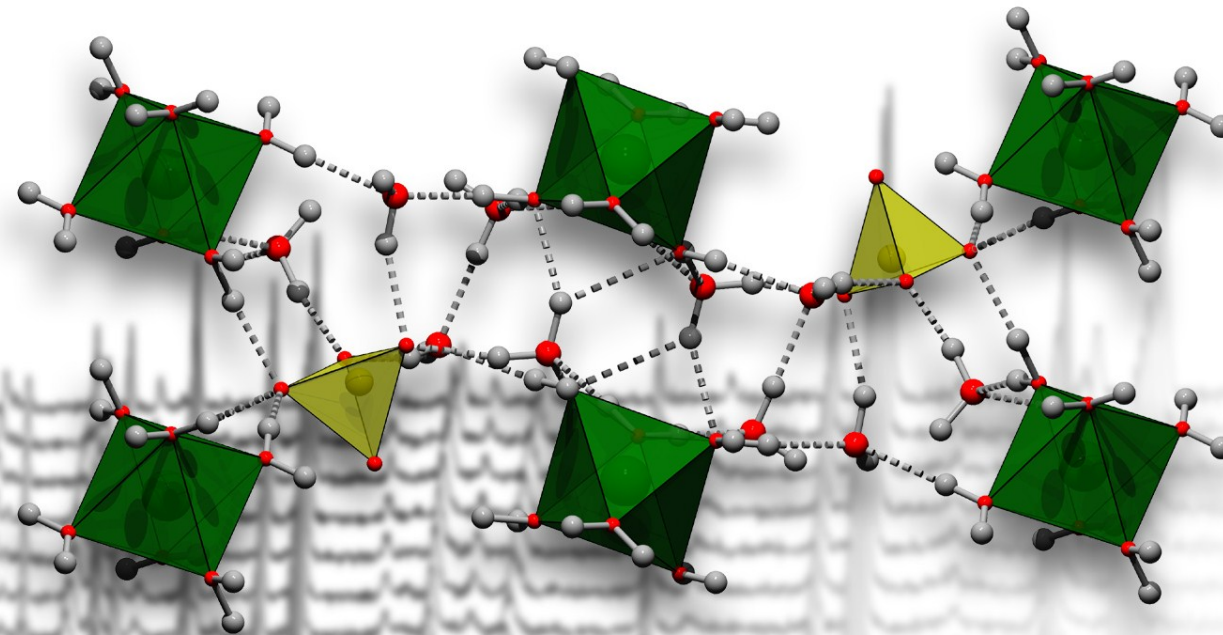


Application of neutron diffraction to planetary ices & hydrates



Dominic Fortes

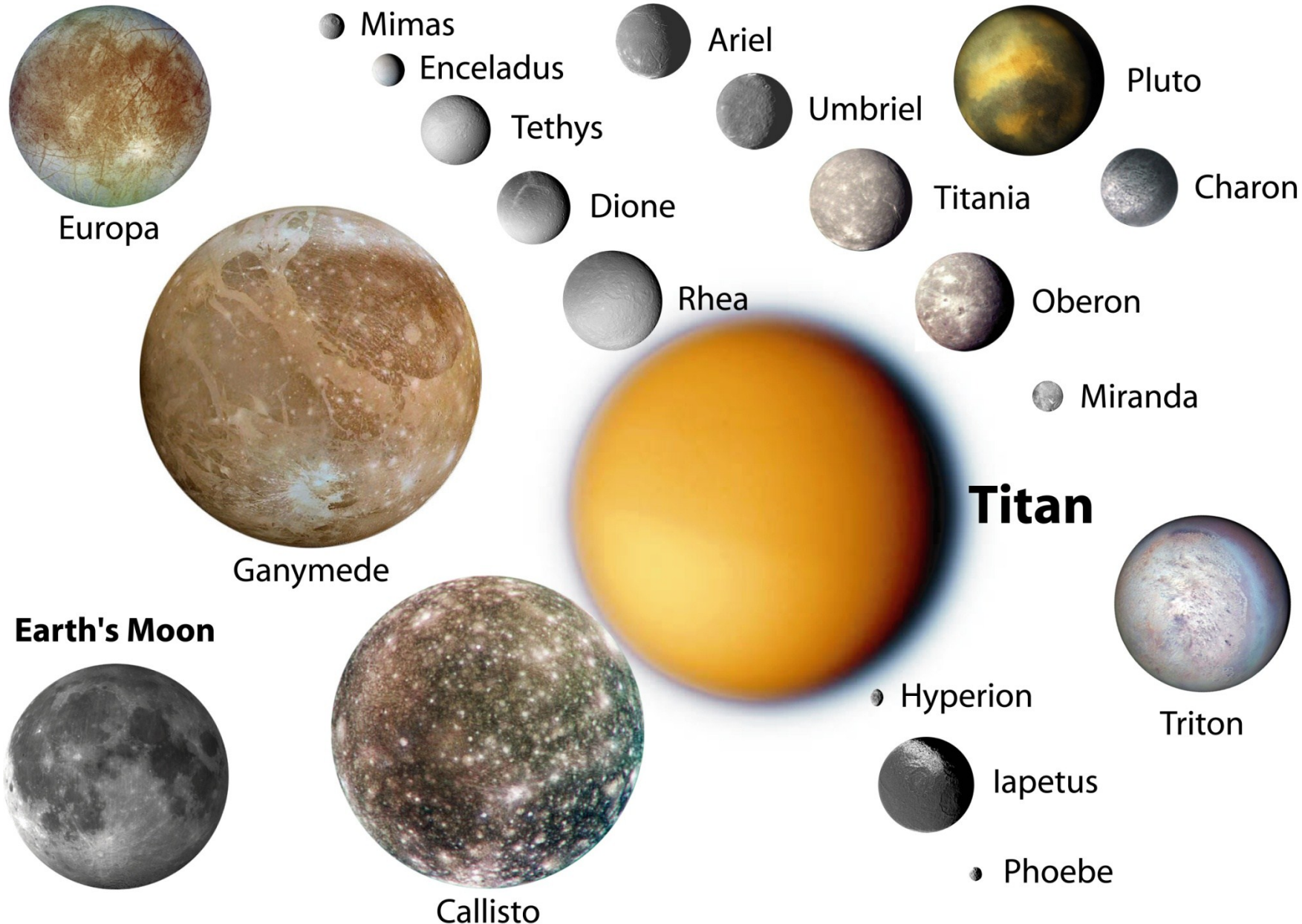
Department of Earth Sciences, University College London



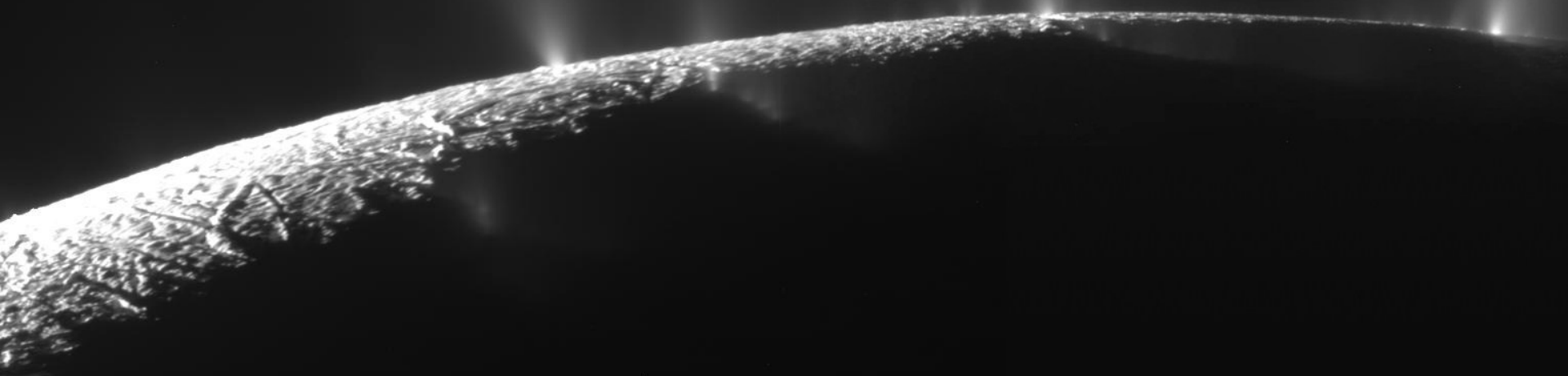
Lecture Outline

1. Introduction – icy bodies of the outer Solar System
What problems do we need to solve, and how can neutrons help us?
2. Materials and methods
3. Some case studies
 - a) High-pressure behaviour of ammonia dihydrate
 - b) High-pressure behaviour of meridianiite ($\text{MgSO}_4 \cdot 11\text{H}_2\text{O}$)
 - c) PVT equation of state of ice VI
 - d) Understanding the thermal expansion of mirabilite ($\text{Na}_2\text{SO}_4 \cdot 10\text{H}_2\text{O}$)

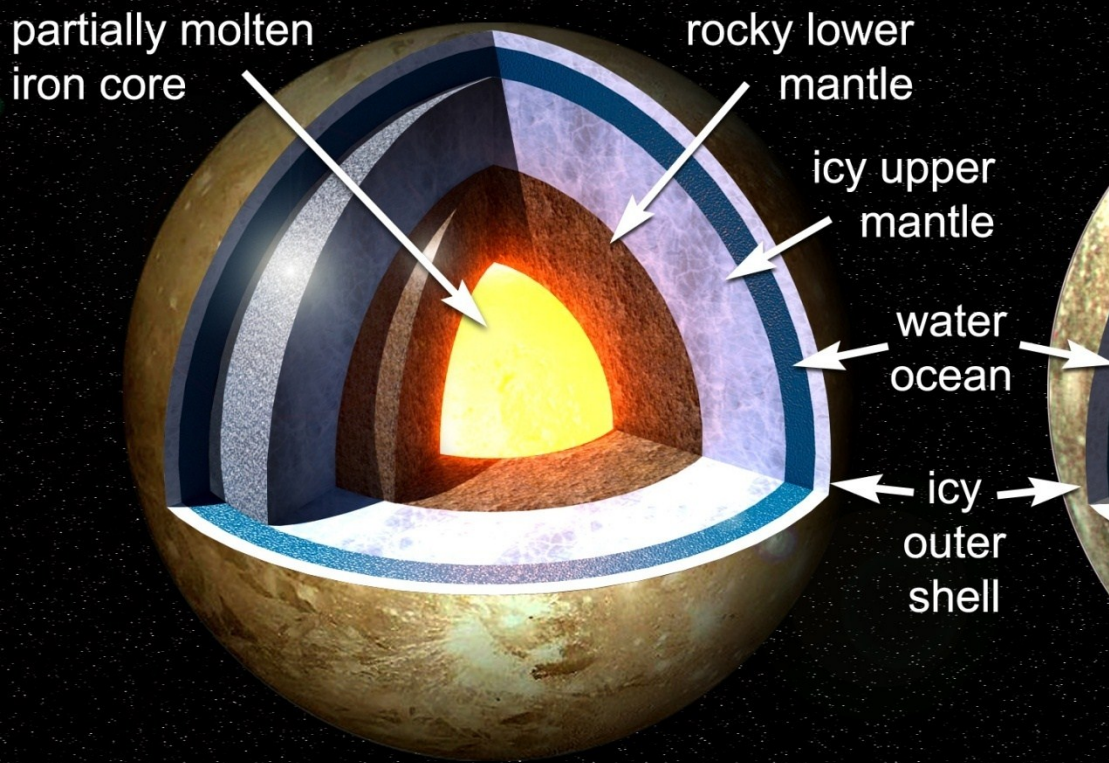
A few icy satellites and planetary bodies



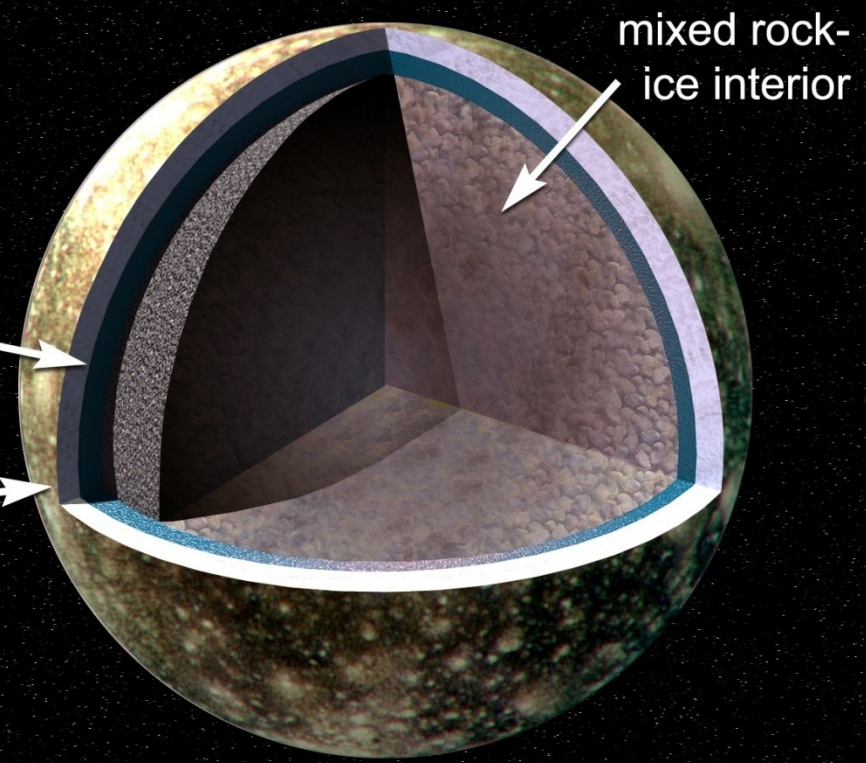
Many icy worlds have been active in the past and some are active even today: Saturn's tiny moon Enceladus erupts ice and water vapour into space at 100s of m/s.



Ganymede



Callisto

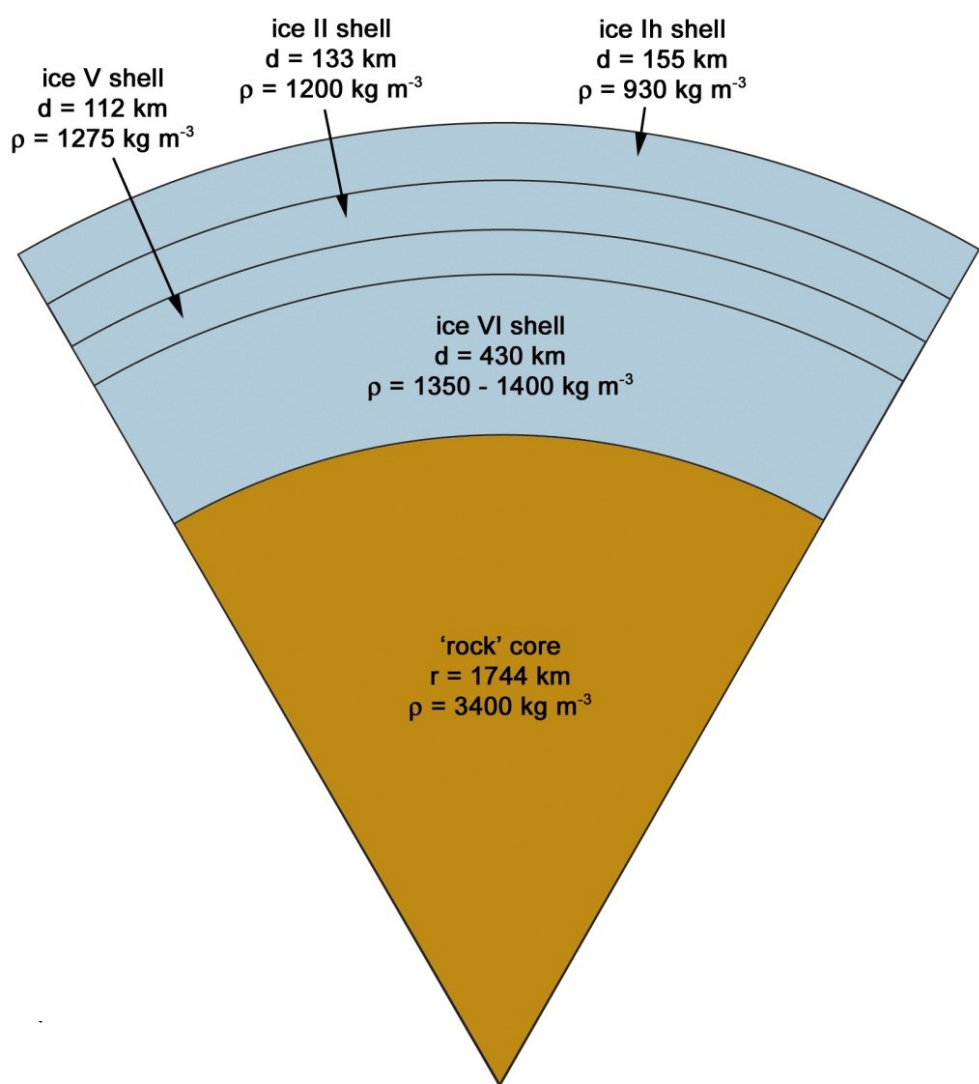
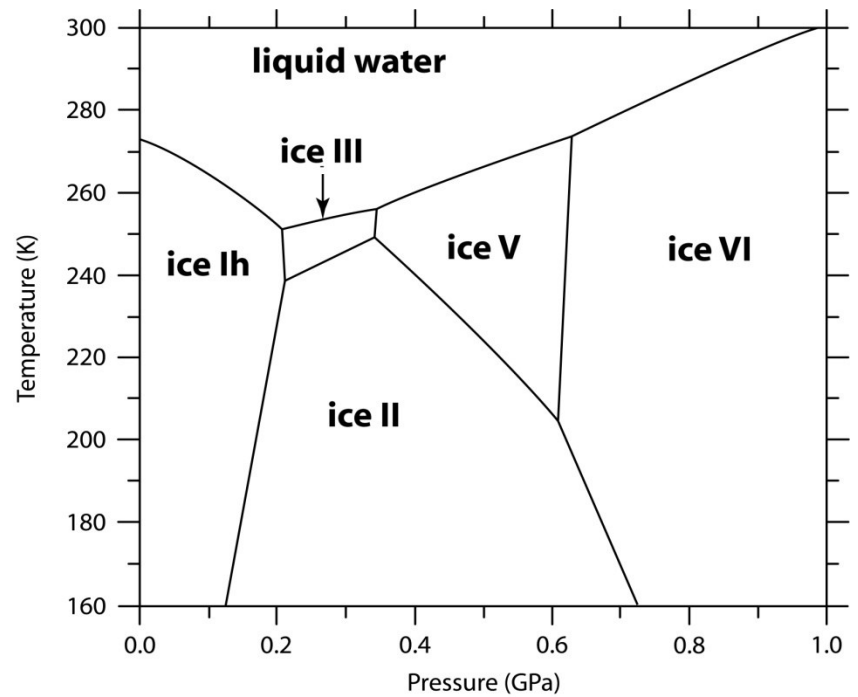


$M_{\text{ol}} = 0.310(3)$

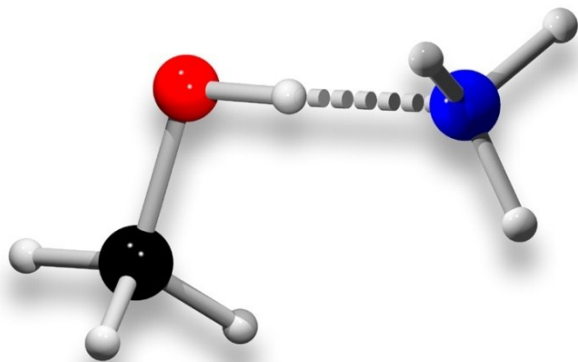
$M_{\text{ol}} = 0.355(4)$

Subsurface oceans are known to exist inside most of the large icy satellites, **Europa**, **Ganymede**, **Callisto** and **Titan**

Modelling structure and thermal evolution



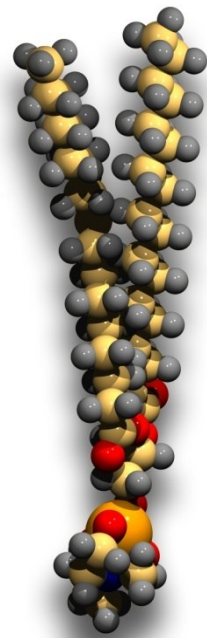
Huaux, A. (1951): Sur un modèle de satellite en glace.
Bulletin de l'Académie Royale des Sciences de Belgique
37, 534-539.



phase
behaviour

crystal
structures

Some applications of neutron diffraction



elastic
properties

astrobiology

rheology

Candidate materials

Primitive volatiles

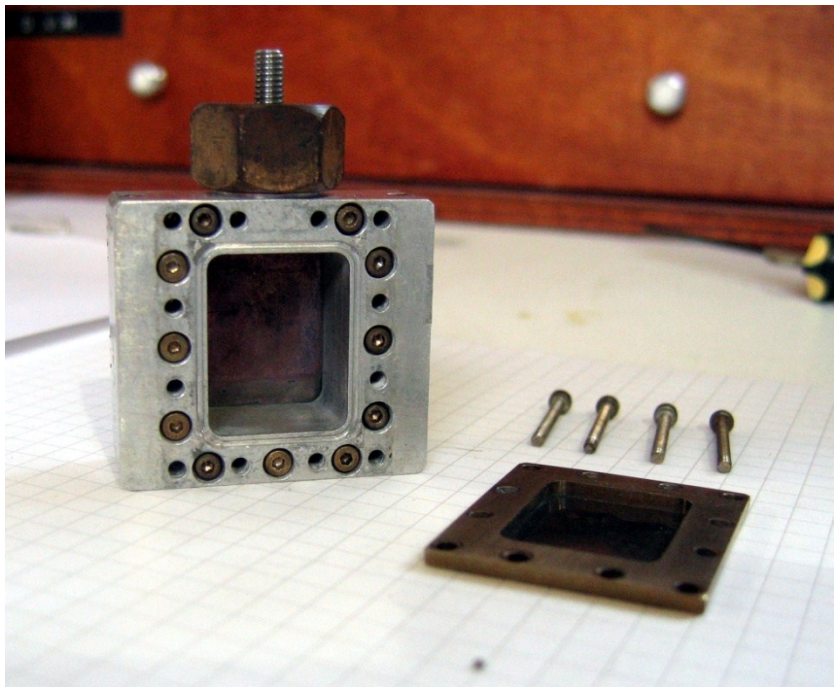


Chondritic salts and acids



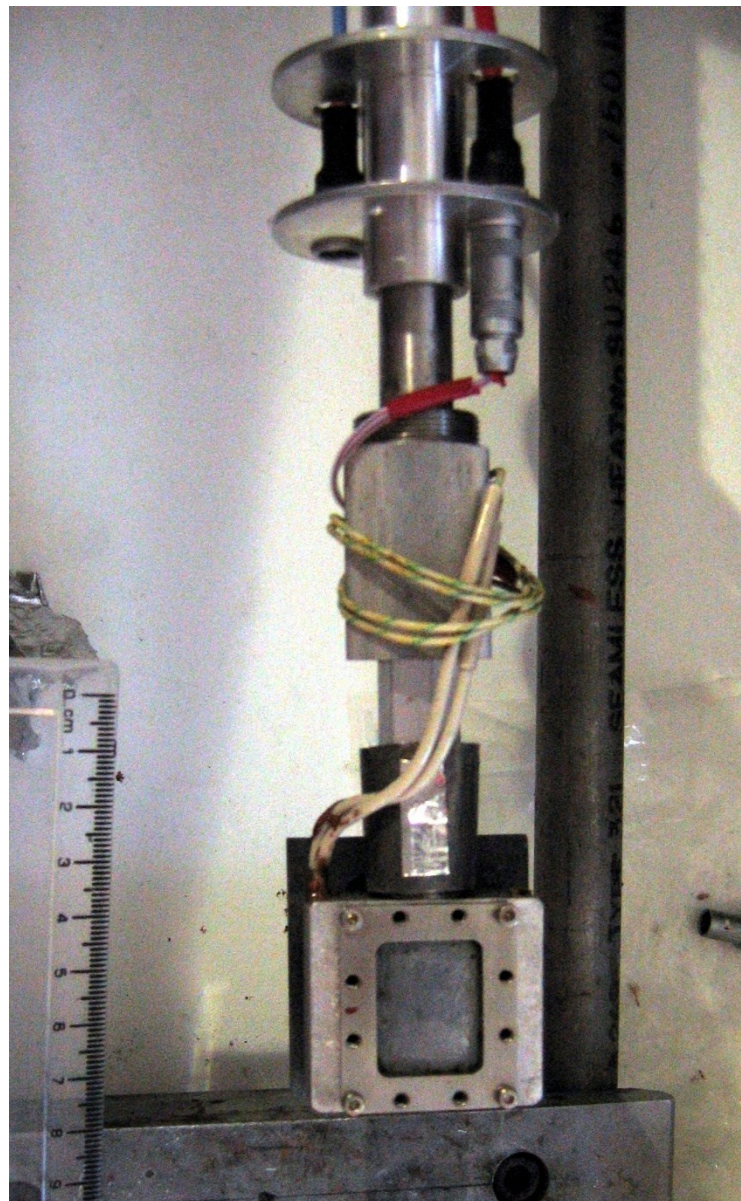
Hydrothermal organics





Low temperature studies are made using an aluminium slab can with vanadium windows.

Sample mass ~ 6 grams
(a bucket-load by X-ray standards)











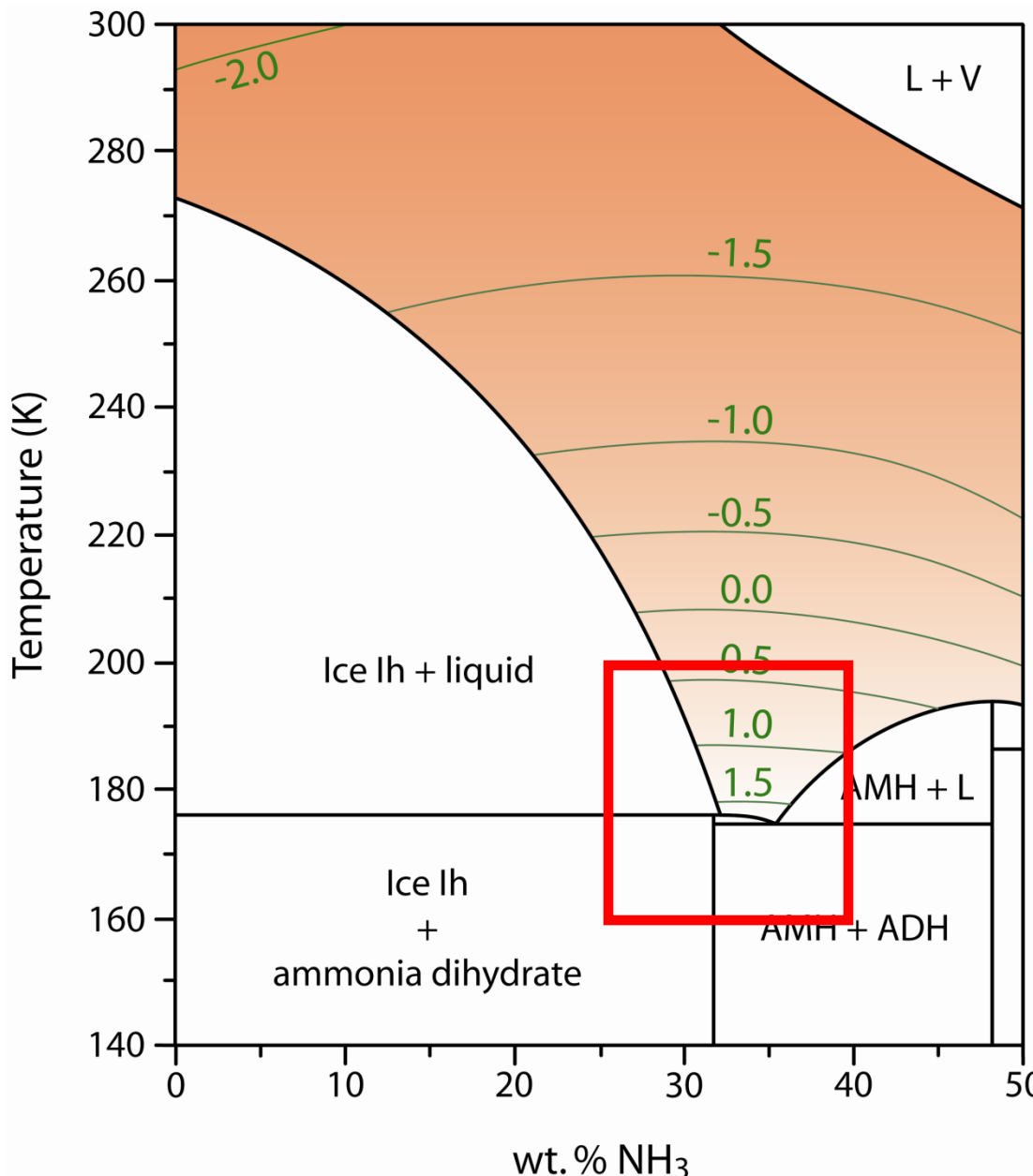






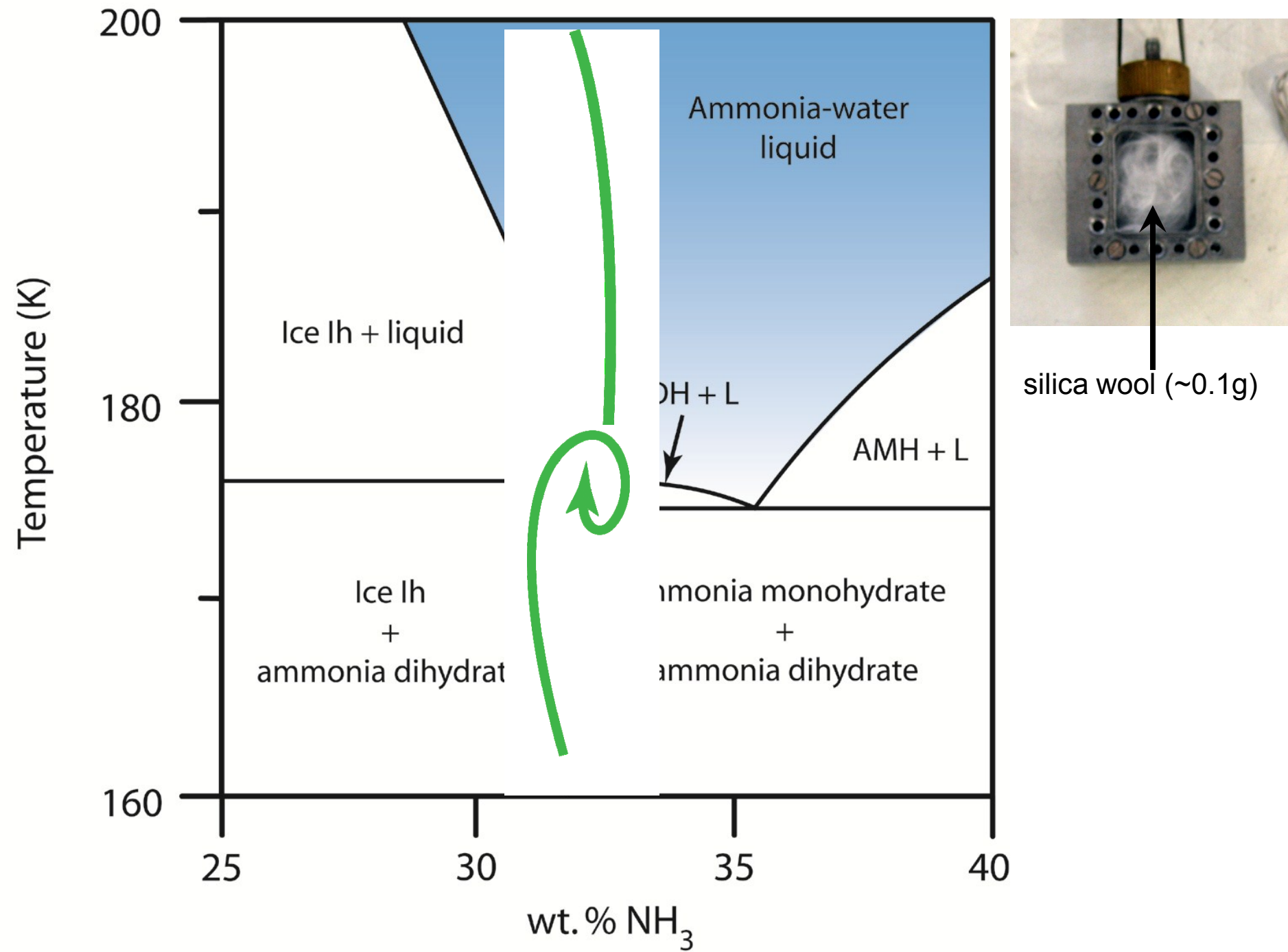


Contours of viscosity (\log_{10} poise) for ammonia-water mixtures



The viscosity of the eutectic solution increases by a factor of more than 6000 on cooling from 295 K to 175 K

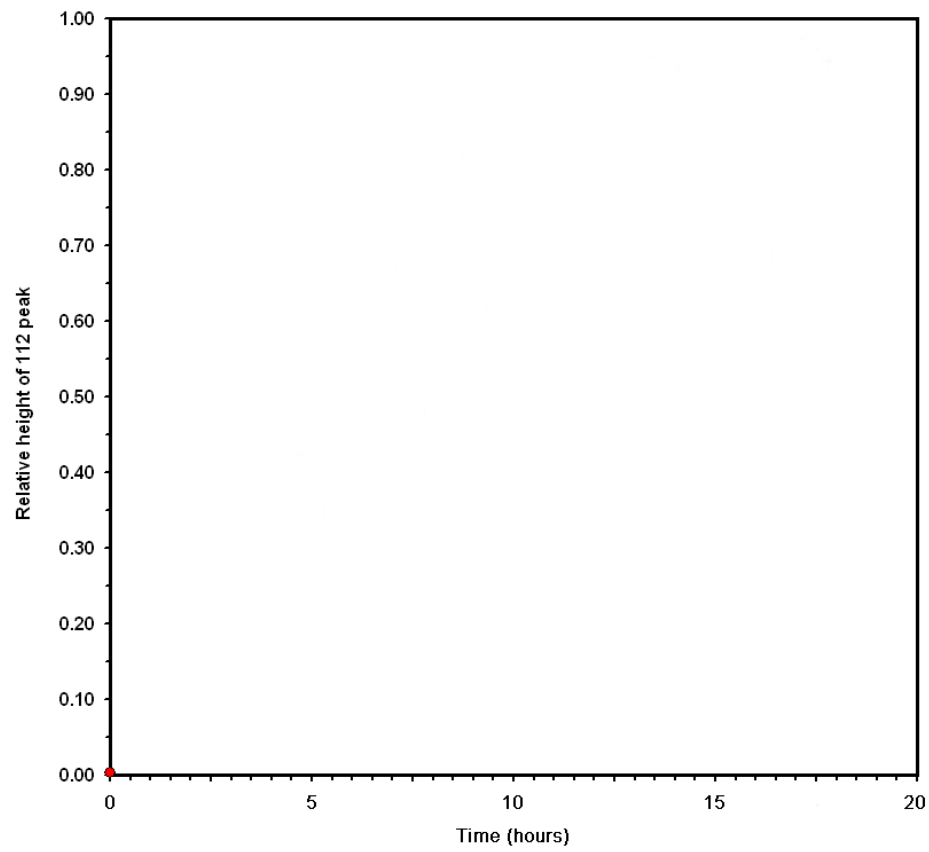
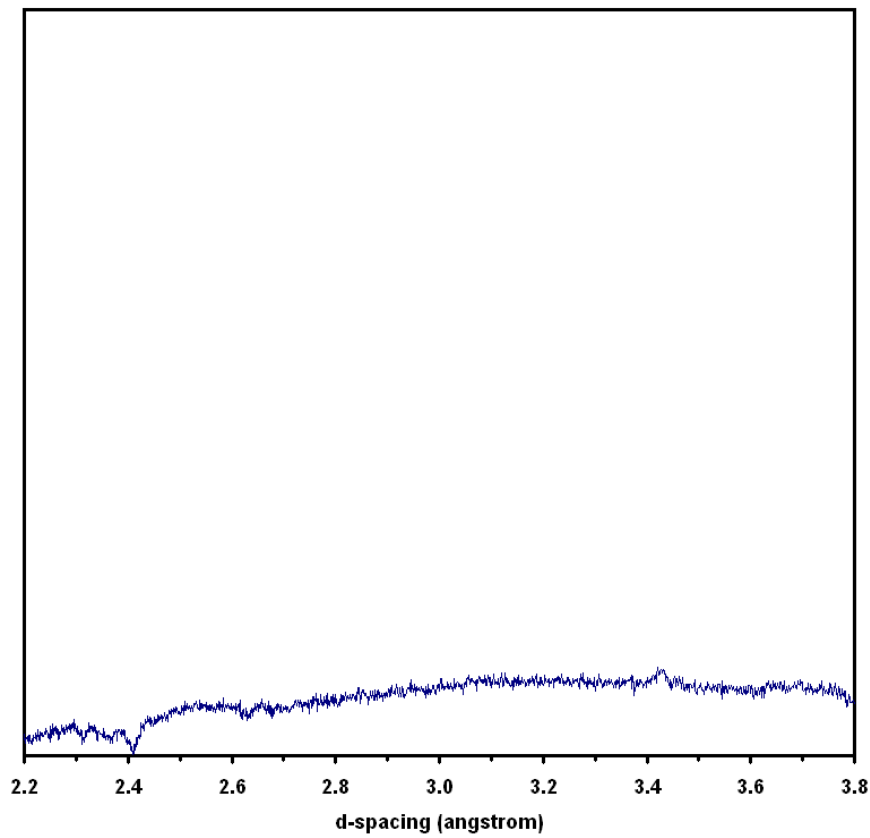




Crystallisation of ammonia dihydrate from glass

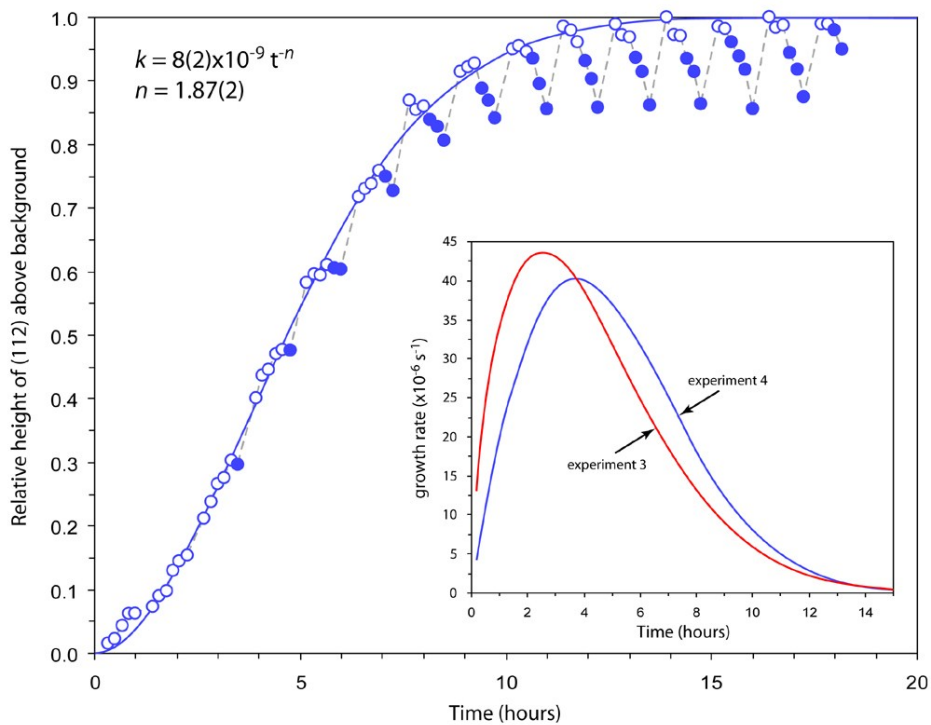
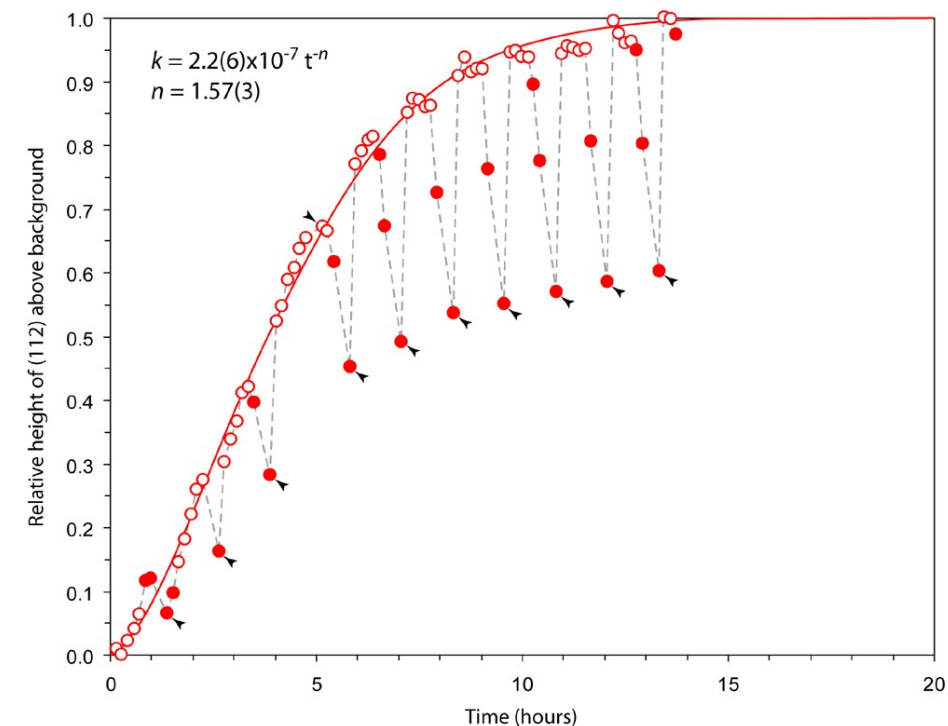
~150 bar; temperature cycled from 173 – 179 K

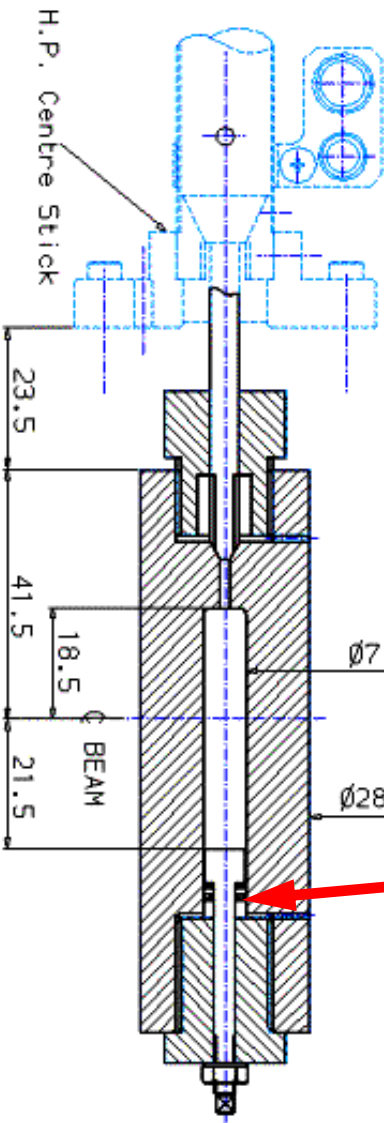
Time dependence of {112} peak height



Crystallisation of ADH as a function of time, fitted with Avrami equation

$$X = 1 - \exp(-kt^n)$$

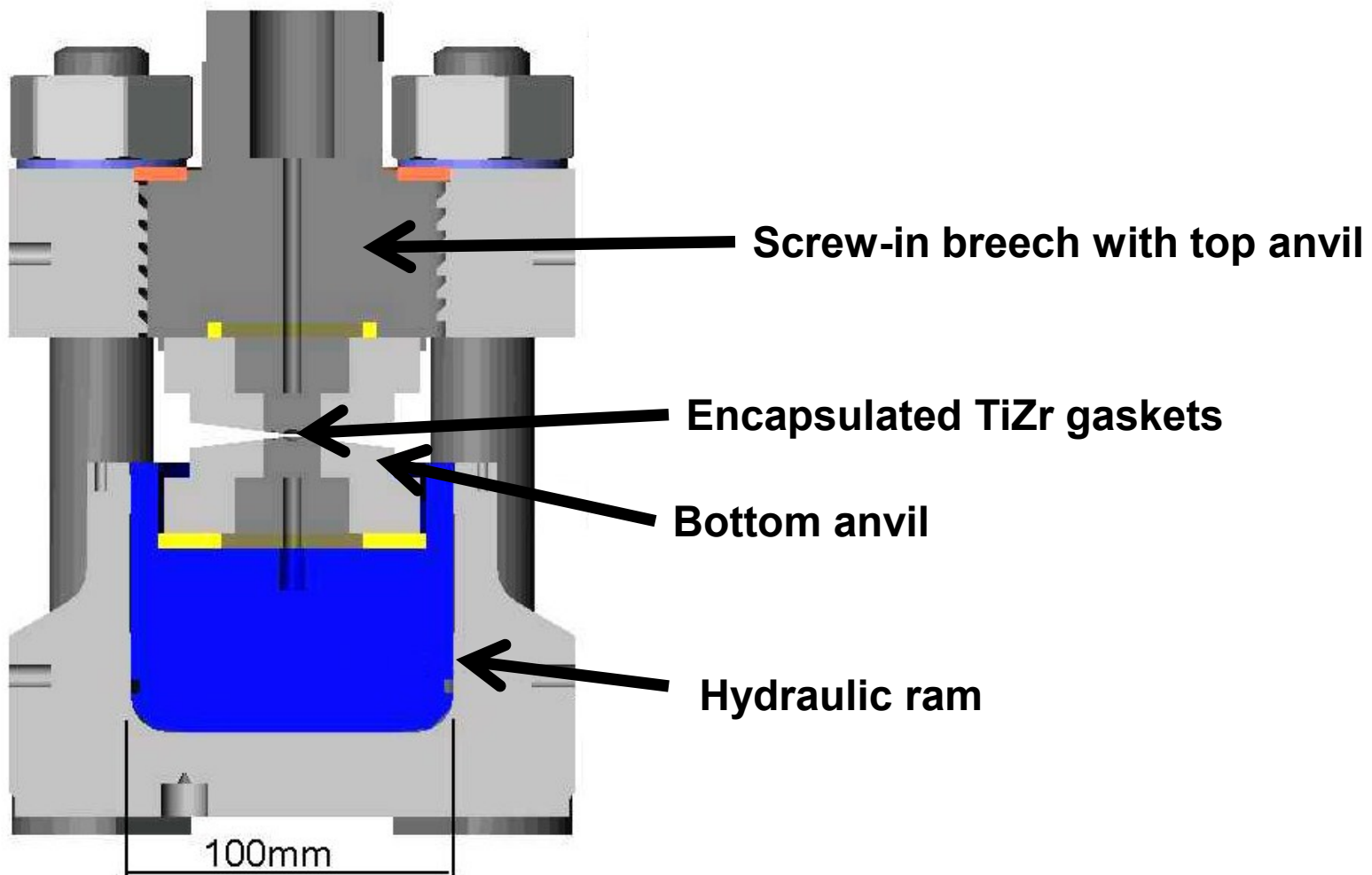




The gas cell design makes a liquid loading unavoidable due to embrittlement of the Bridgman seal at low-T
Al and TiZr gas cell sample volume $\sim 1.5 \text{ cm}^3$

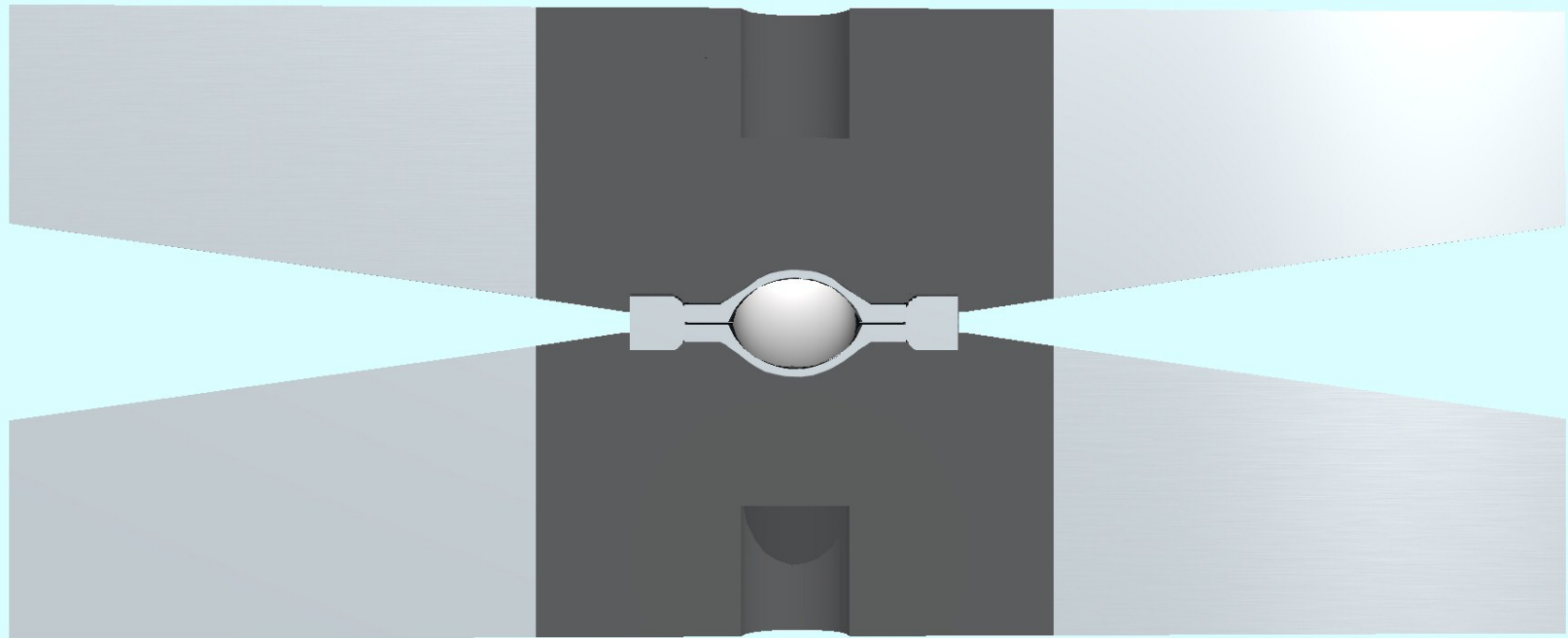
Higher-P sample environment

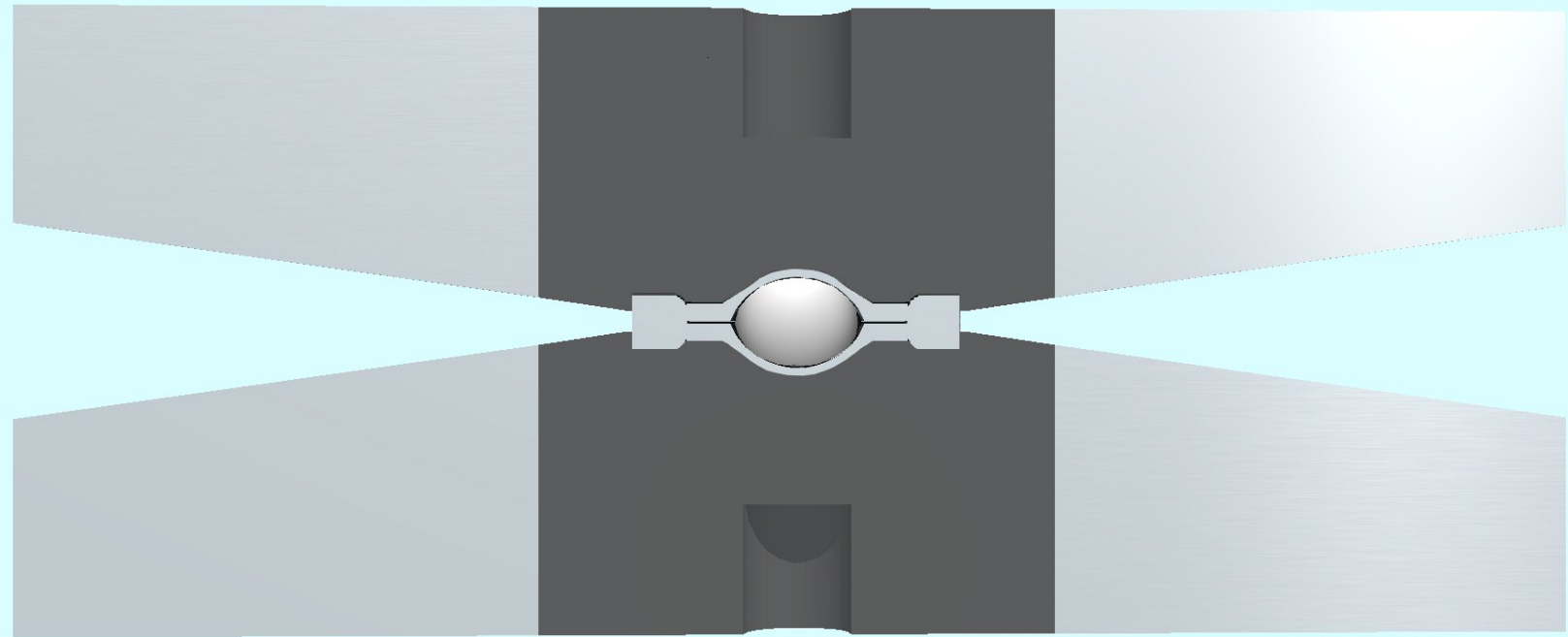
Paris-Edinburgh large-volume press (0 – 10 GPa)



Sample mass ~ 100 mg

For cold loading of solids, need to keep ~ 100 kg of metal cold.





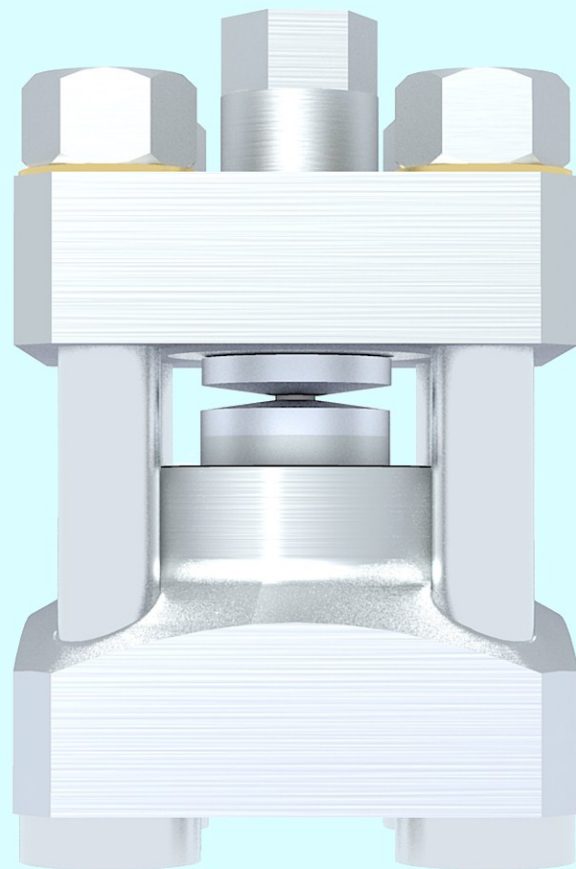
a

PARIS-EDINBURGH HYDRAULIC PRESS

oreech

anvil set

h

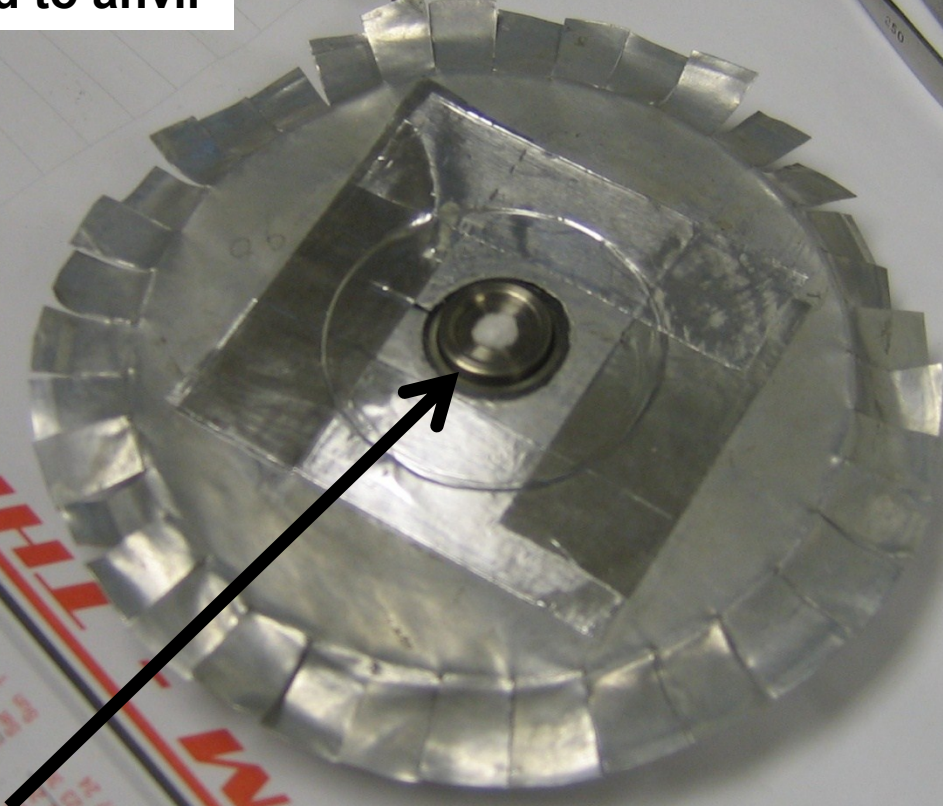


pillars

Paris-Edinburgh cell anvil

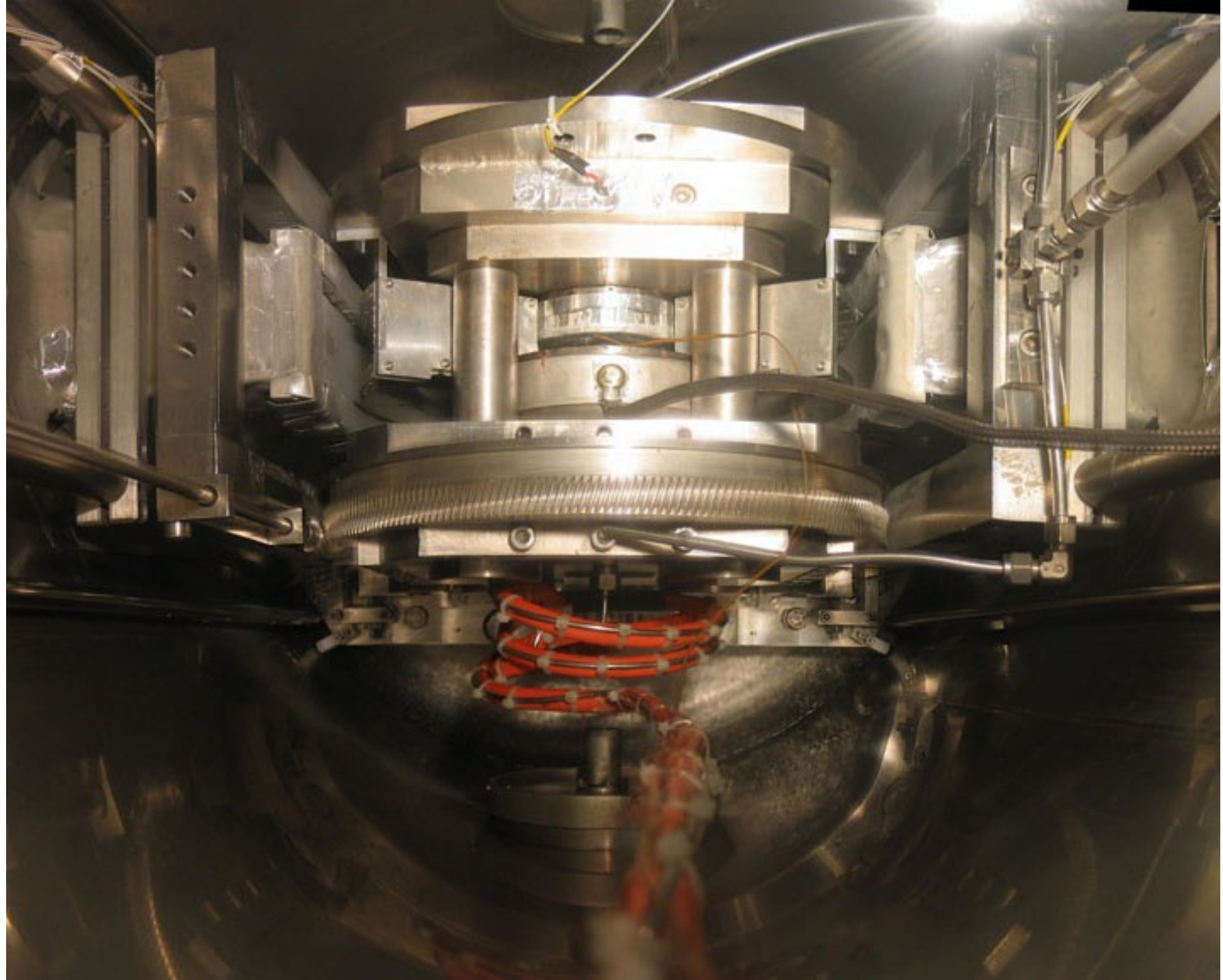
Tungsten-carbide, coated with cadmium

Thermocouple taped to anvil



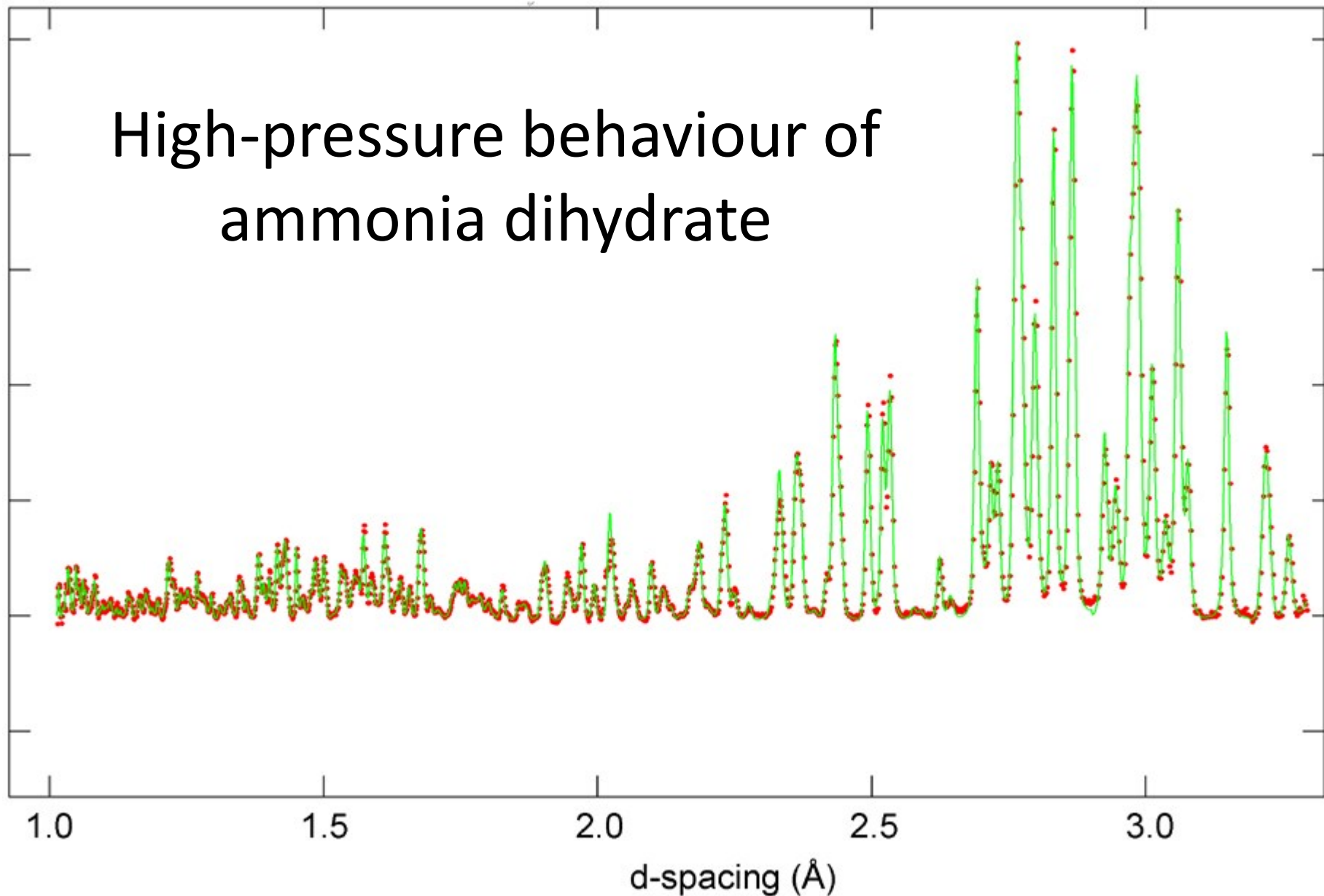
Encapsulated TiZr gasket, filled with
silica wool, containing a ball of Pb foil



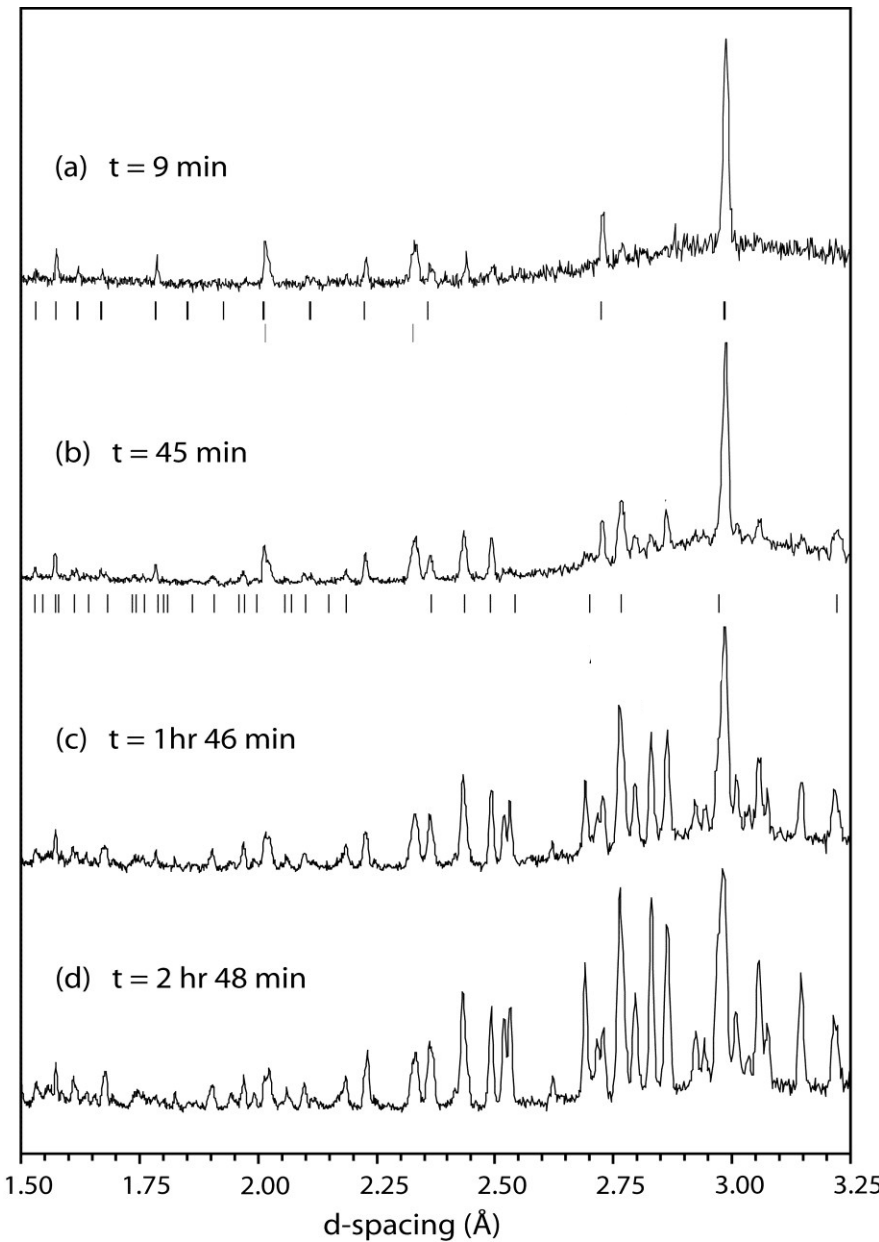


Case study 1:

High-pressure behaviour of ammonia dihydrate



Growth of a phase mixture at high pressure



Re-crystallisation sequence at
174 K at \sim 450 MPa

ice IX + liquid



growth of ice II

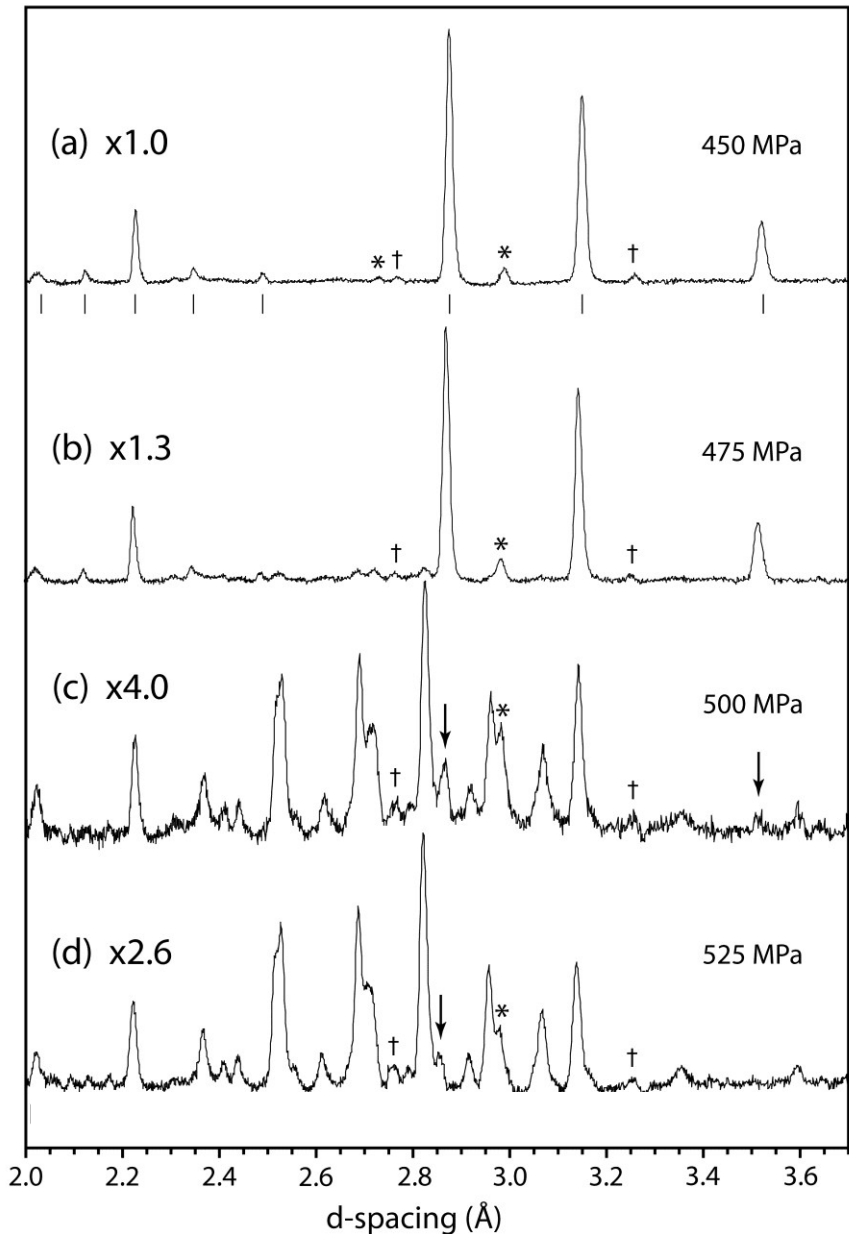


growth of ammonia hydrate(s)

ammonia dihydrate II
+

ammonia monohydrate II

Isothermal compression through a phase transition



Phase transition in ammonia dihydrate upon compression from 0.1 – 525 MPa

cubic phase I of ADH



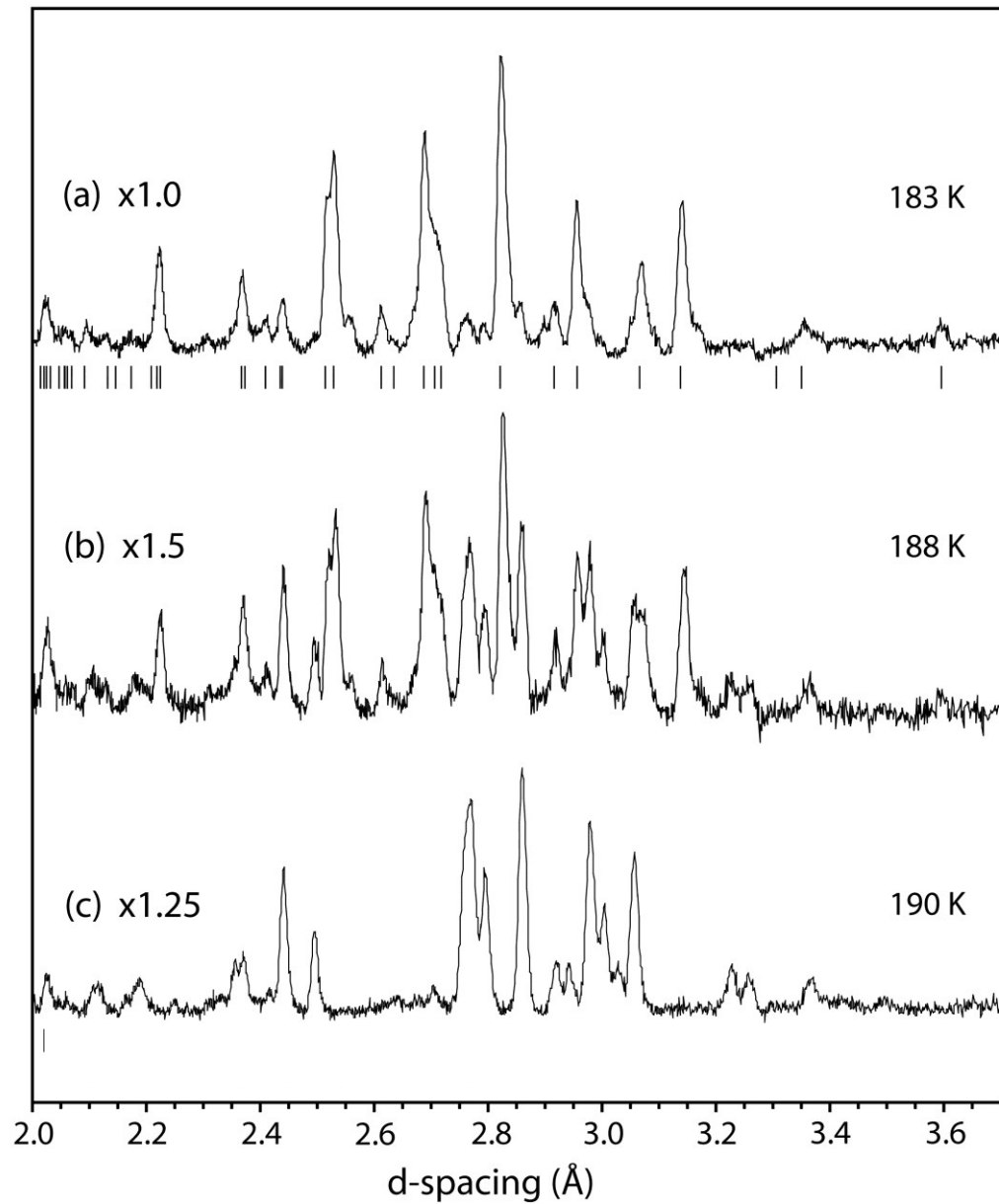
phase II of ADH

ADH II (monoclinic)
 $a = 7.7686(11)$ Å
 $b = 6.6947(11)$ Å
 $c = 6.0380(8)$ Å
 $\beta = 101.967(14)$ °

$P = 546$ MPa, $T = 173$ K
 $V = 307.20$ Å³ ($Z = 4$)
 $M(11) = 97.1$
 $F(11) = 97.2$ (0.0039, 29)

Systematic absences indicate space-groups, Pn, P2/n, or P2₁/n

Isobaric warming through a phase transition



Phase transition in ADH
upon warming at 550 MPa

monoclinic phase II of ADH
(ADH II)



mono-phase, multi-phase???

Partial melting under high pressure

Partial melting of AMH + ice mixture
upon warming at 550 MPa

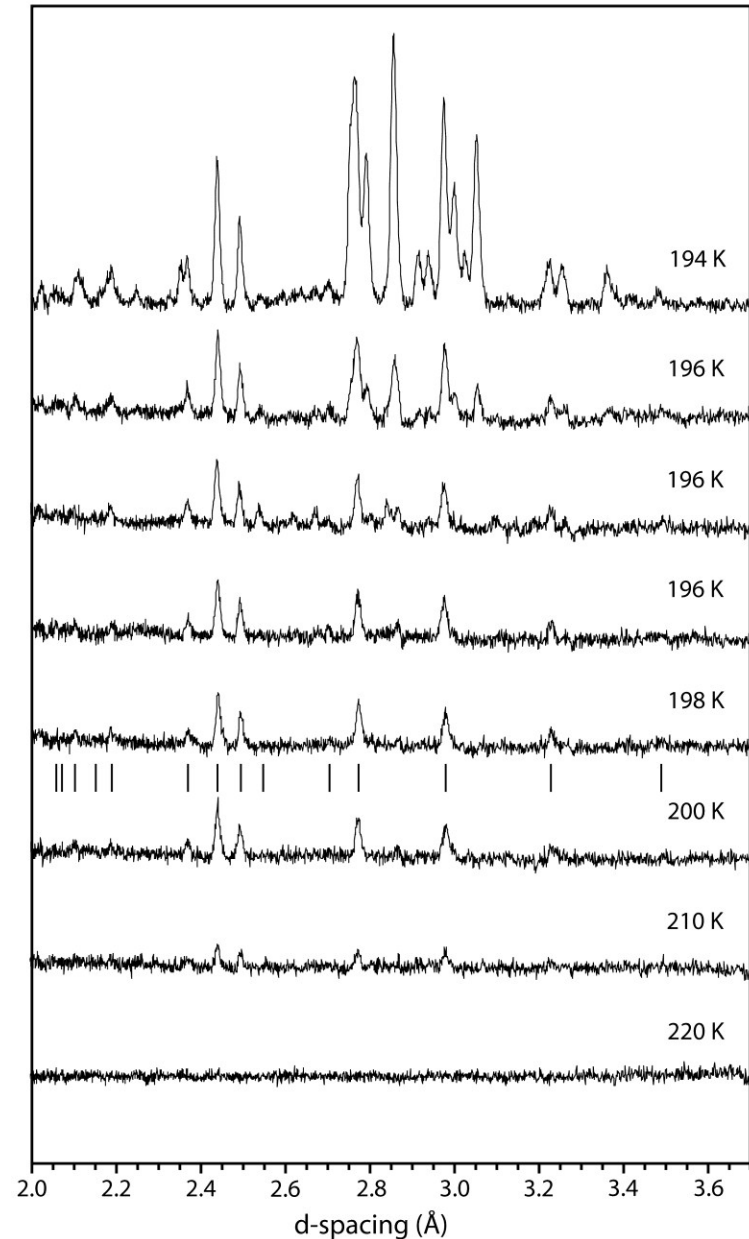
AMH II + ice II



ice II + liquid



liquid



Powder indexing and solution of AMH II structure

AMH II (orthorhombic)

$a = 18.8119(33) \text{ \AA}$

$b = 6.9400(10) \text{ \AA}$

$c = 6.8374(8) \text{ \AA}$

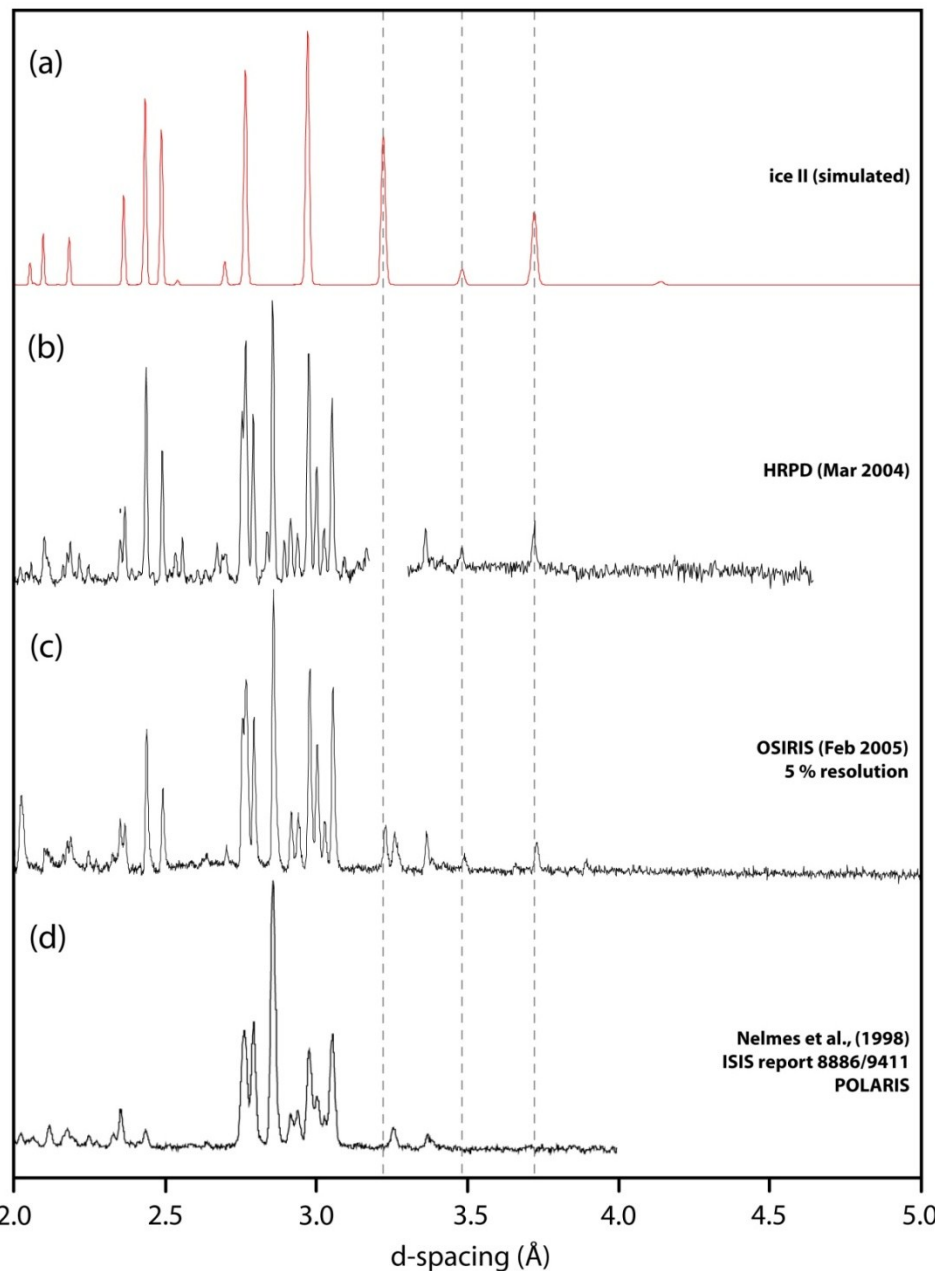
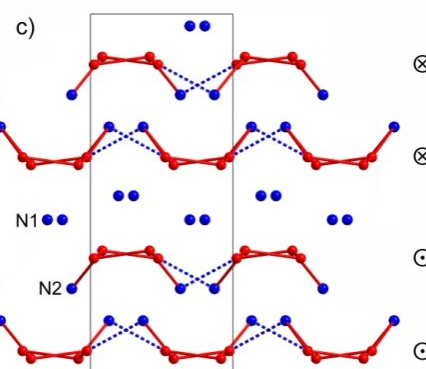
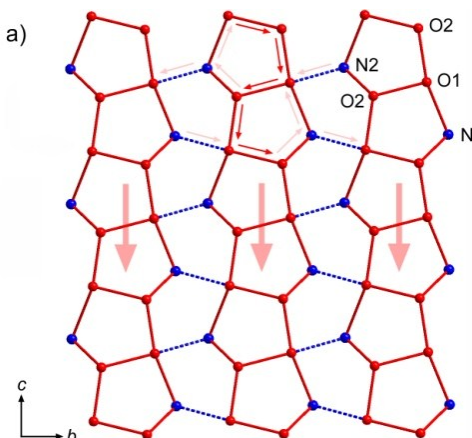
$P = 550 \text{ MPa}, T = 190 \text{ K}$

$V = 892.66 \text{ \AA}^3 (Z = 16)$

$M(12) = 51.5$

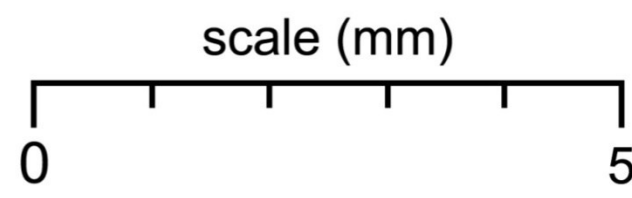
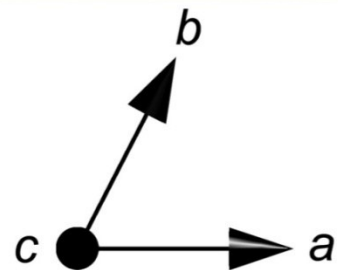
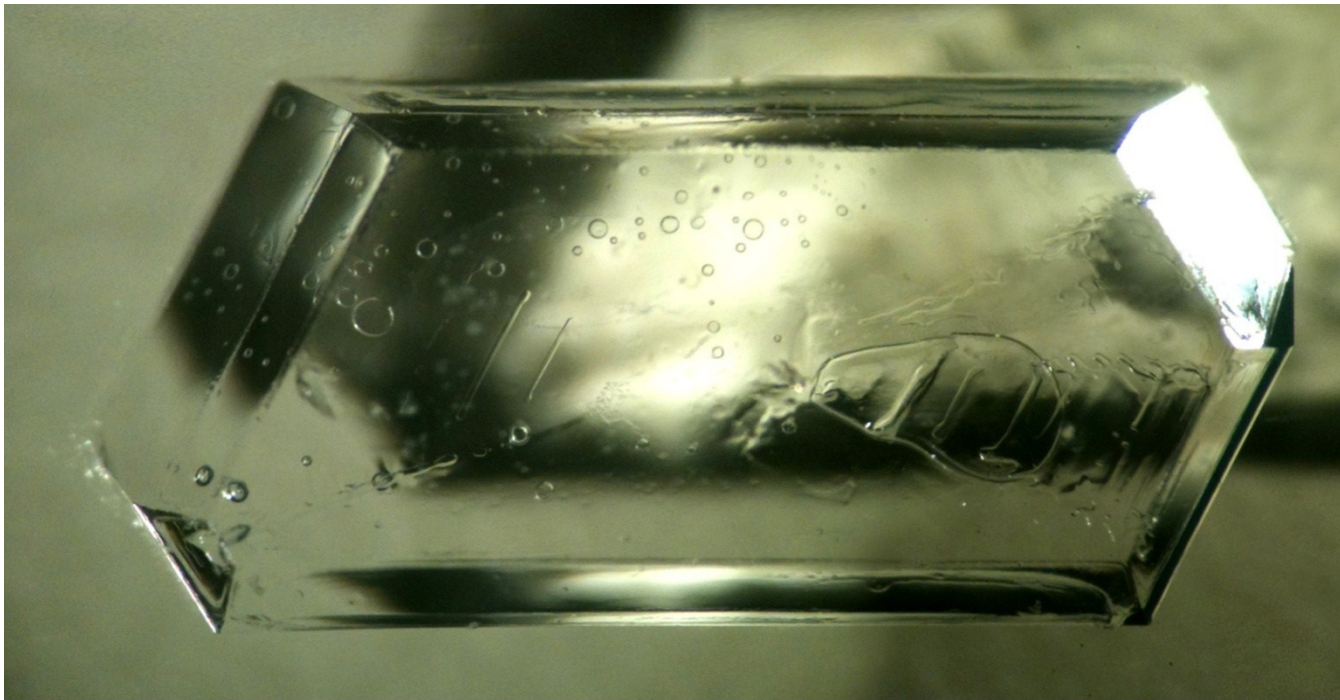
$F(12) = 65.7 (0.0041, 44)$

Structure subsequently solved in space-group Pbca. Consists of a pentagonally tessellated net similar to that found in tetragonal argon clathrate.



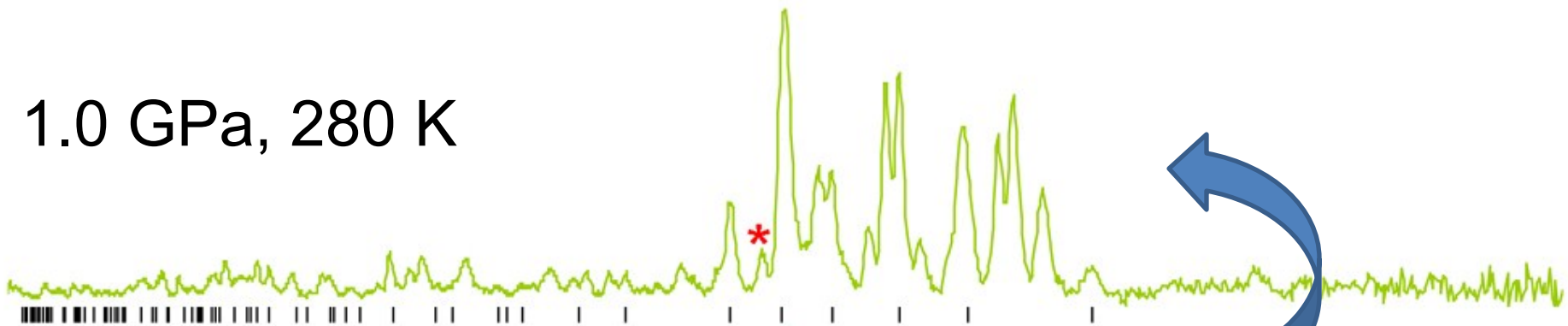
Case study 2:

The high-pressure behaviour of meridianiite

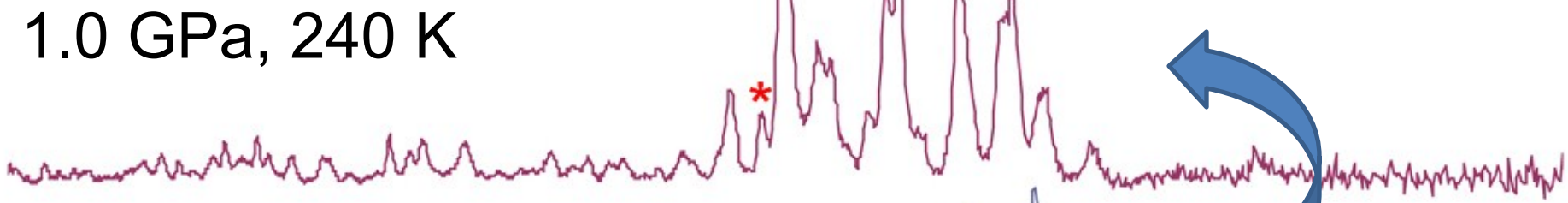


High-pressure transformation of meridianiite

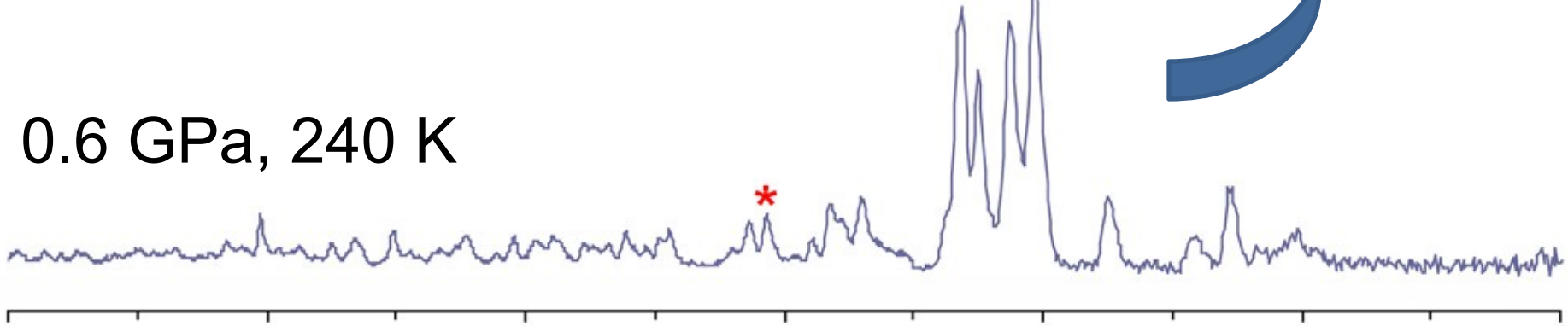
1.0 GPa, 280 K



1.0 GPa, 240 K



0.6 GPa, 240 K



d-spacing (\AA)

1.0

1.5

2.0

2.5

3.0

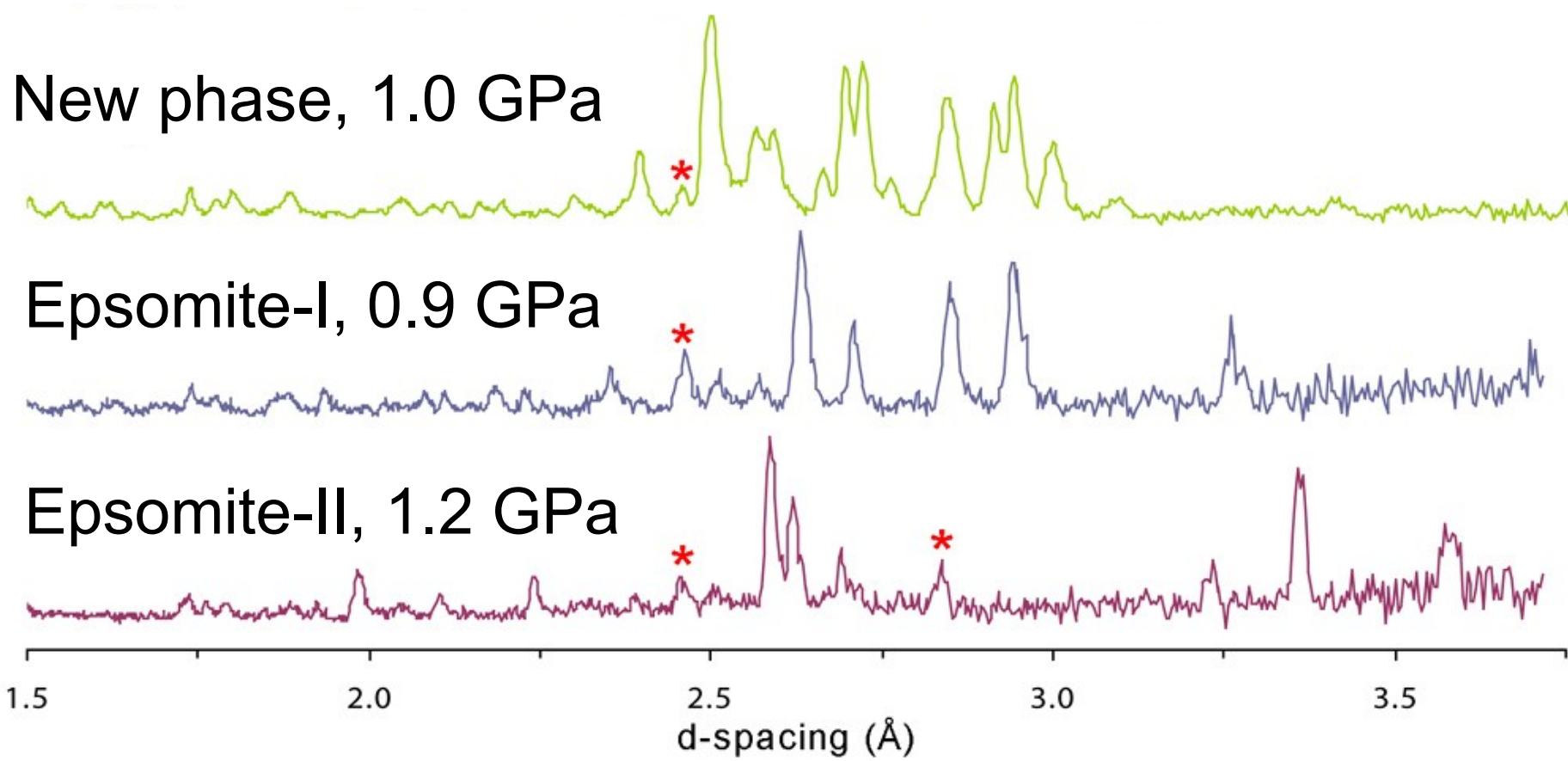
3.5

4.0

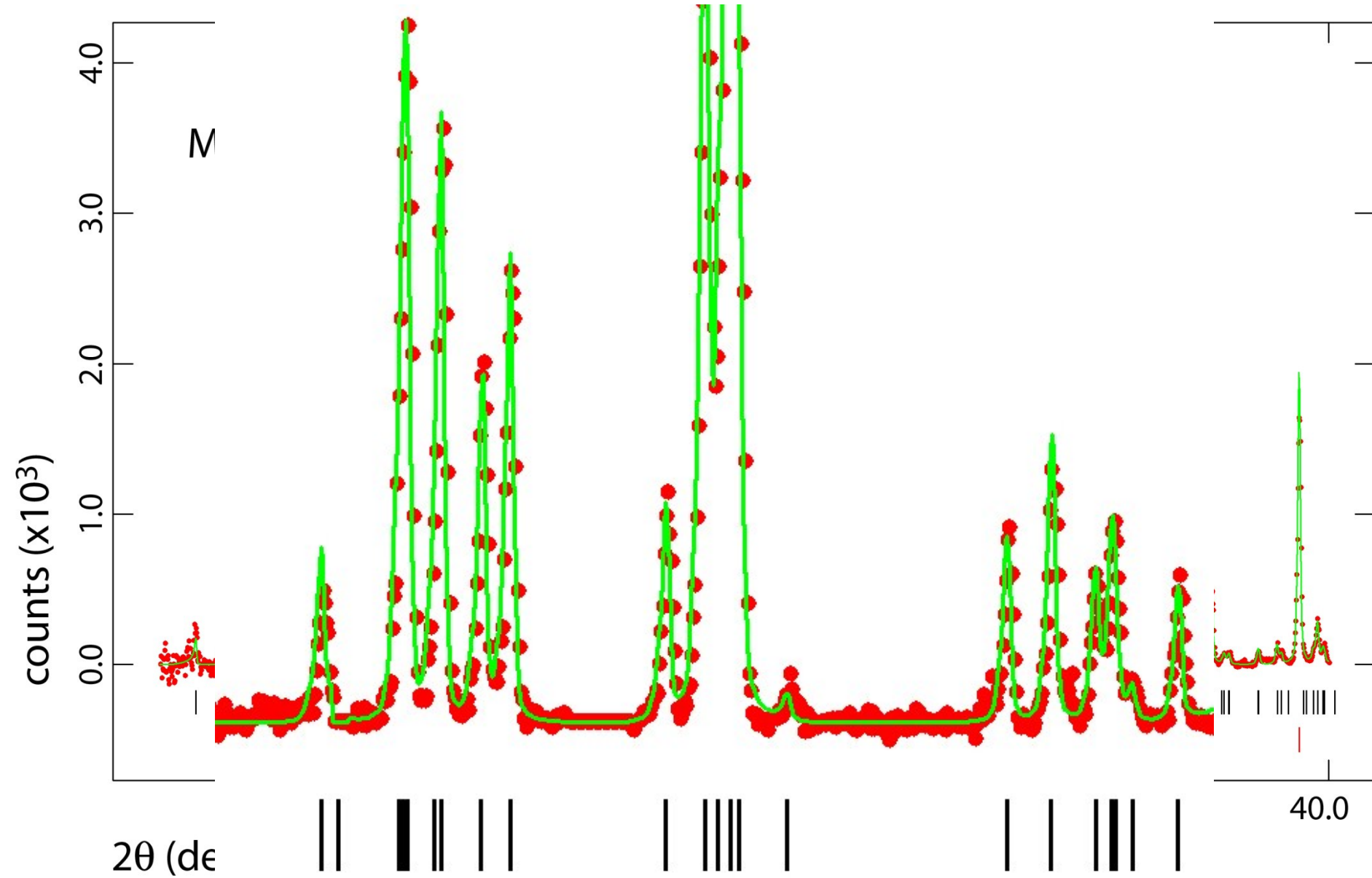
The exsolution of ice indicates a change in hydration state

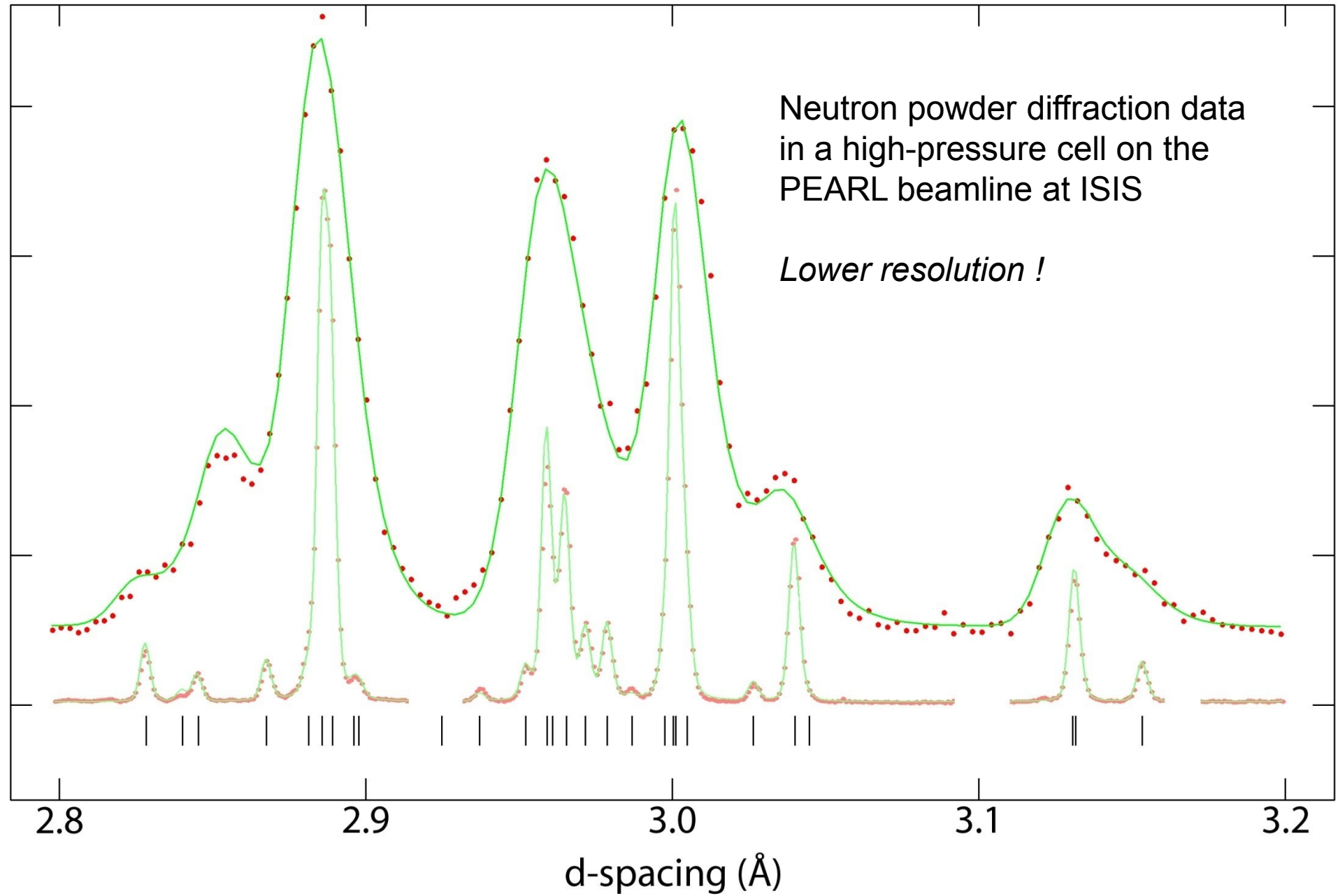
No obvious match to epsomite at high-pressure

Suggests that the new phase has a hydration state between 7 and 11



High resolution X-ray powder data from a laboratory diffractometer
essential for indexing unknown phases





One solution to this problem is to seek structural analogues with different compositions, which might form novel hydrates under conditions where we can acquire high-resolution data.

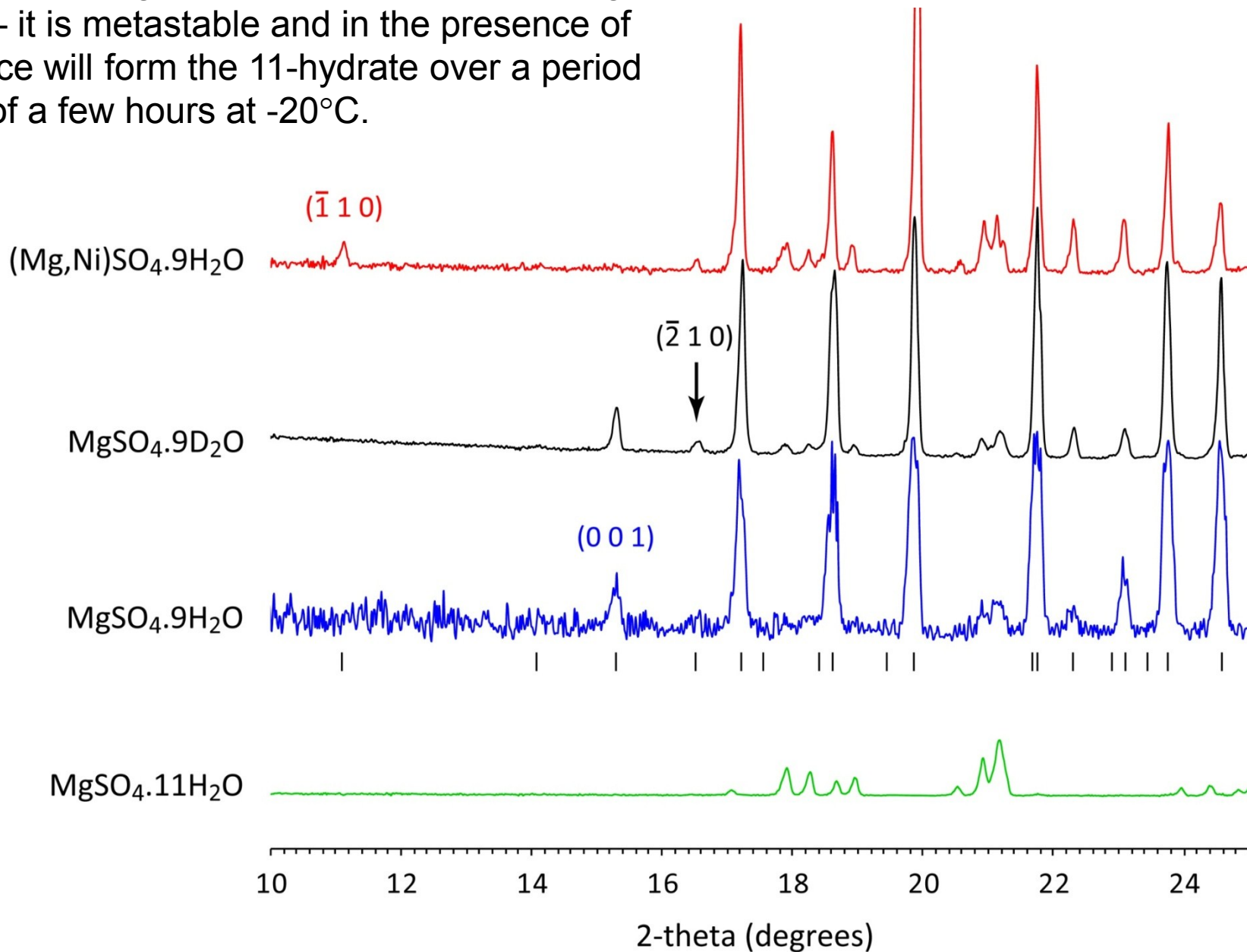
A.D. FORTE

Occurrence of known $\text{MgX}^{6+}\text{O}_4 \cdot n\text{H}_2\text{O}$ crystals

$n =$	4	5	6	7	8	9	10	11
SO_4	✓	✓	✓	✓		✓		✓
SeO_4	✓	✓	✓	✓		✓		✓✓
TeO_4				work in progress				
CrO_4		✓		✓		✓		✓
MoO_4		✓		✓	✓			
WO_4		✓		✓	only amorphous solids so far			

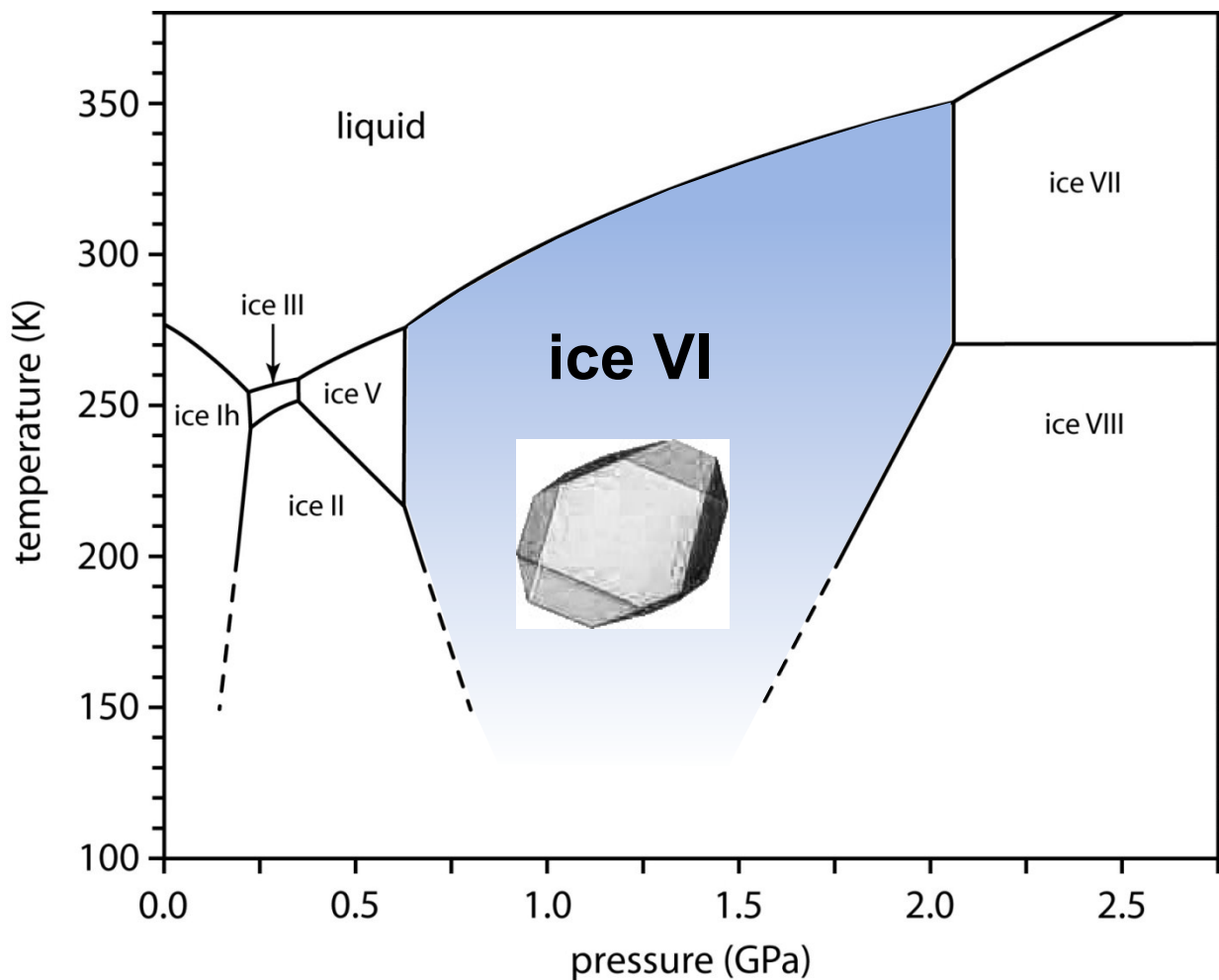
$\text{MgSeO}_4 \cdot 9\text{H}_2\text{O}$ is particularly interesting because this phase seems to be stable in aqueous solution, although it is not isostructural with any of the other 9-hydrates identified so far.

Pure MgSO_4 9-hydrate can be formed by quenching small droplets in liquid nitrogen – it is metastable and in the presence of ice will form the 11-hydrate over a period of a few hours at -20°C .



Case study 3:

P-V-T equation of state of ice VI



inter-planar spacing (angstrom)

1.0 1.5 2.0 2.5 3.0 3.5

counts per microsecond

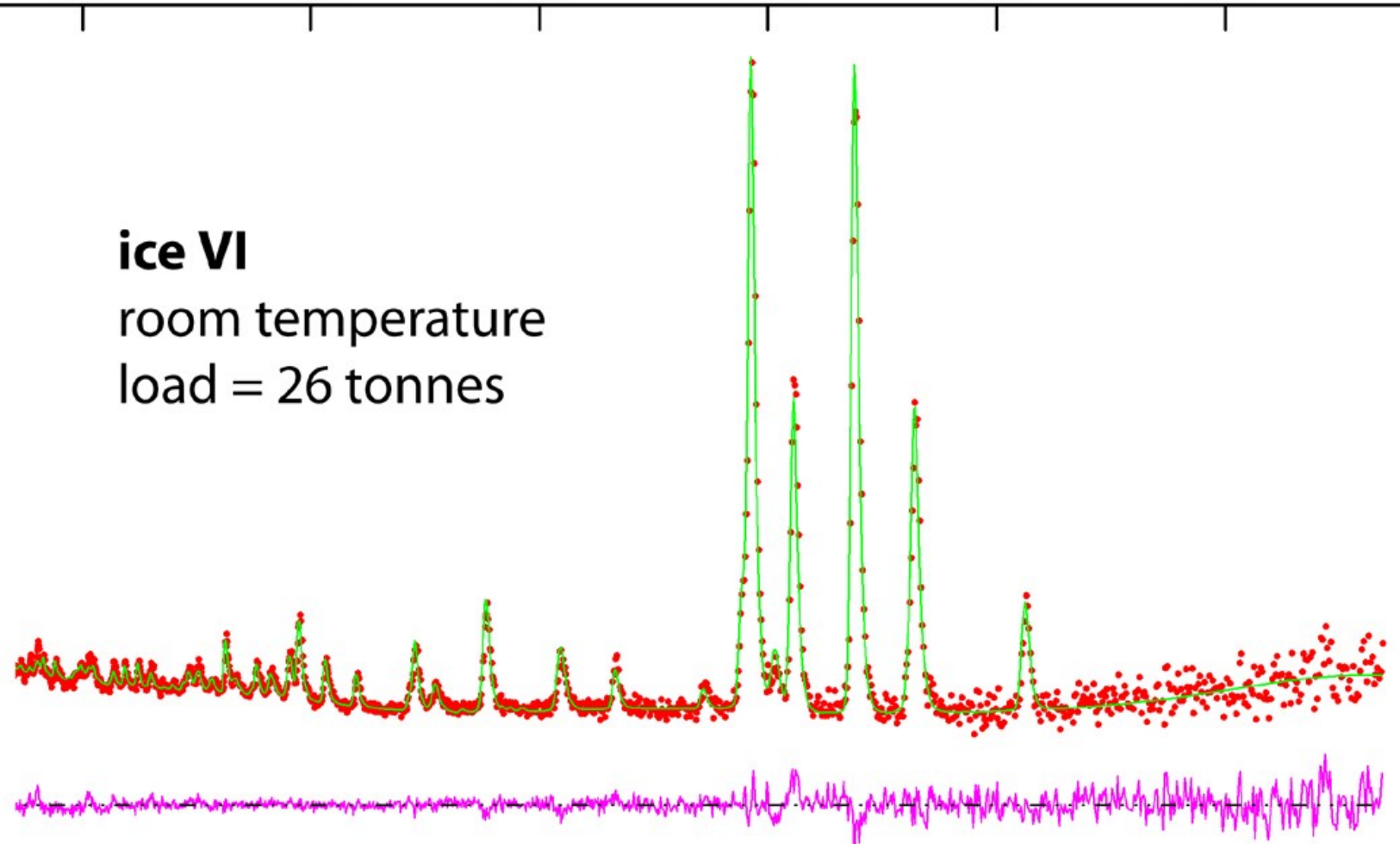
8.0
6.0
4.0
2.0
0.0

ice VI

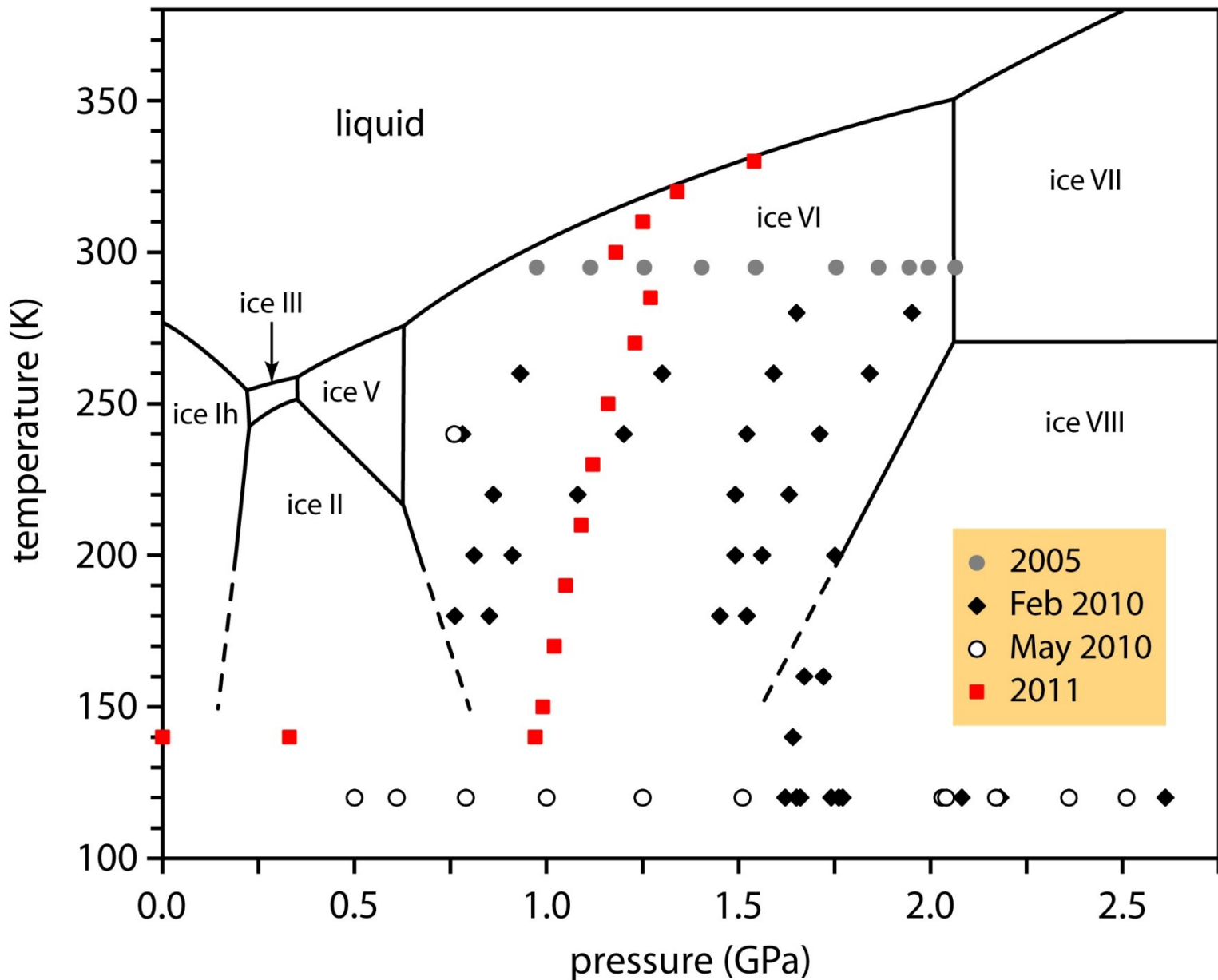
room temperature
load = 26 tonnes

4.0 6.0 8.0 10.0 12.0 14.0 16.0 18.0

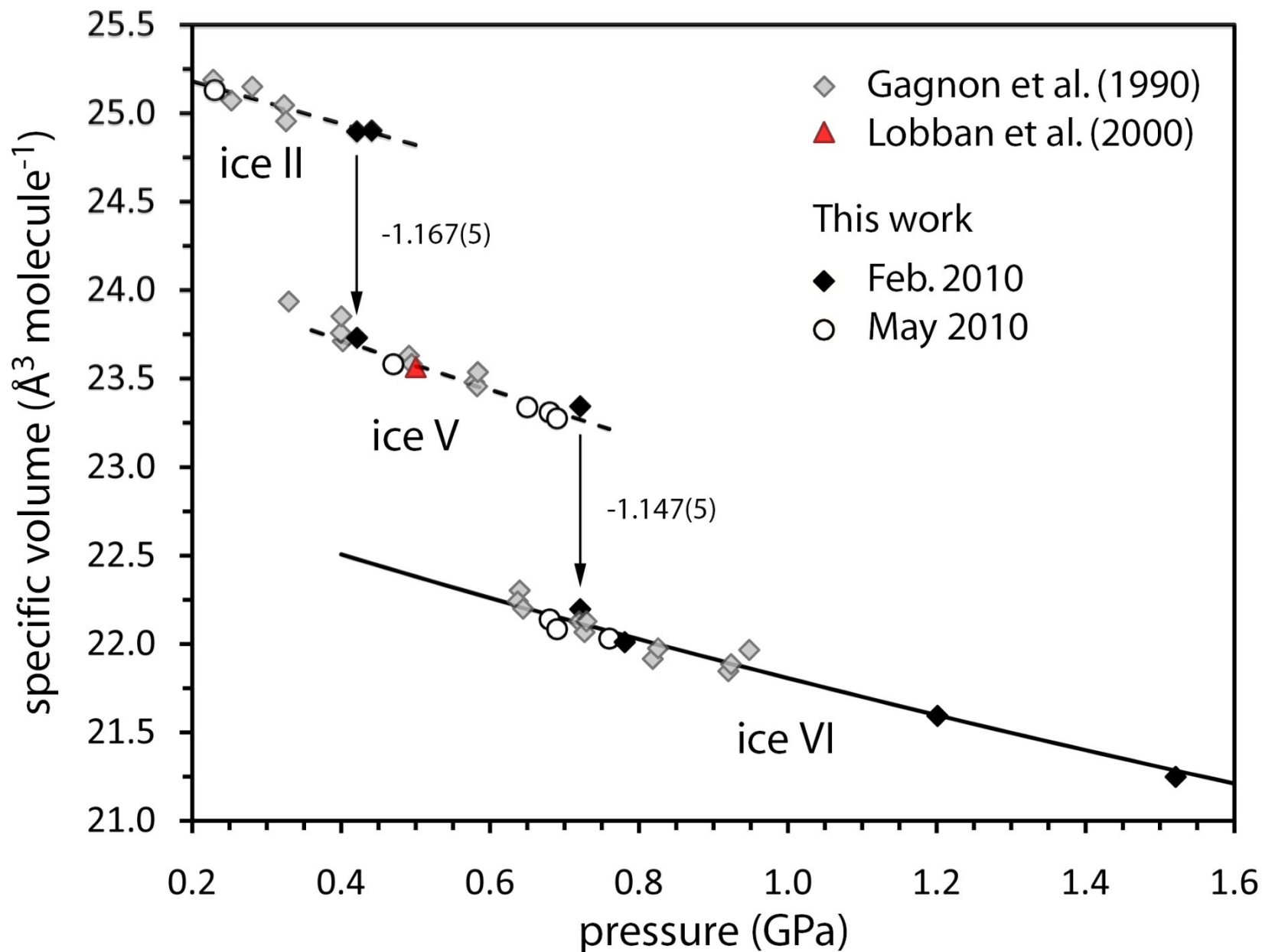
neutron time-of-flight (msec)



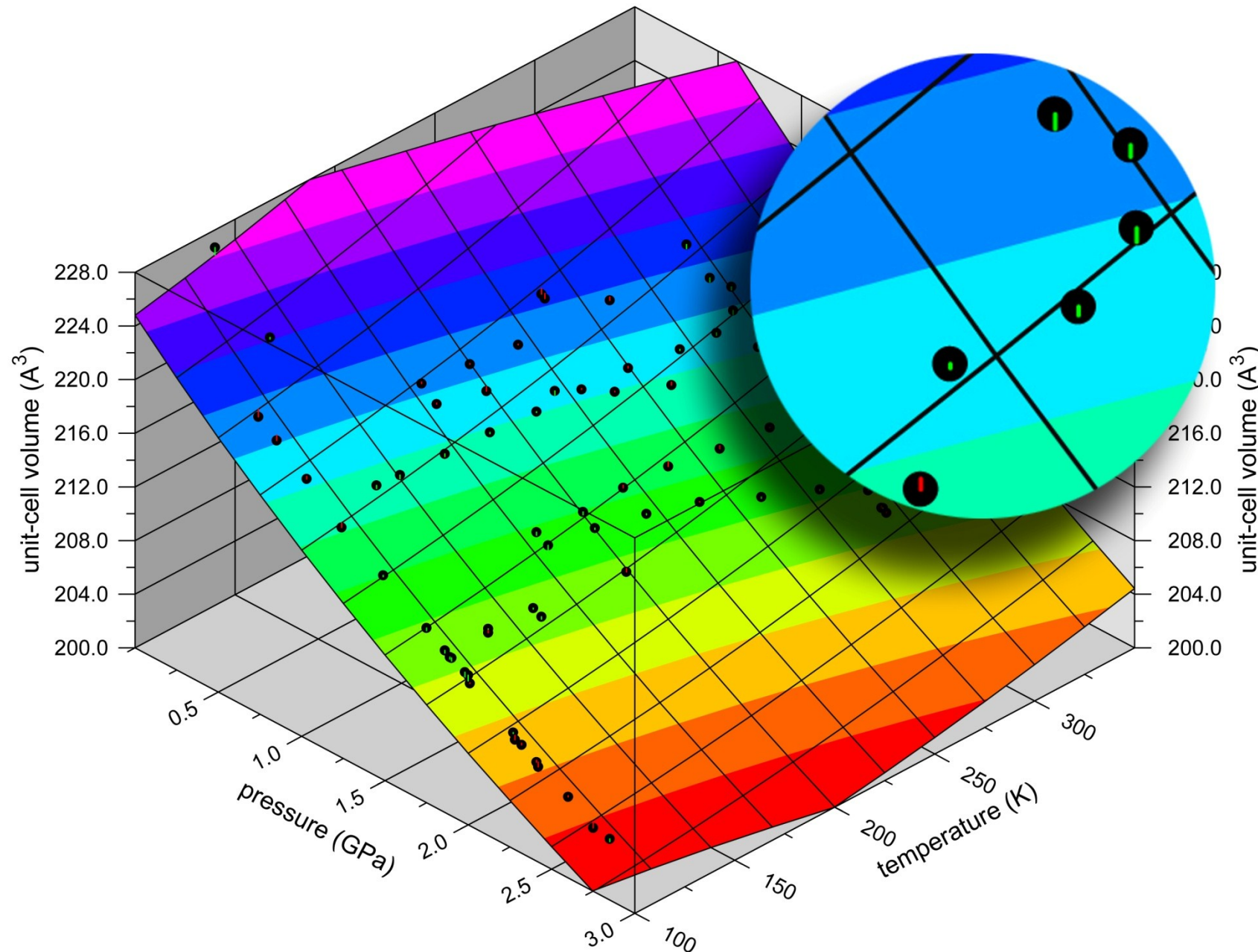
P-T distribution of measurements on ice-VI



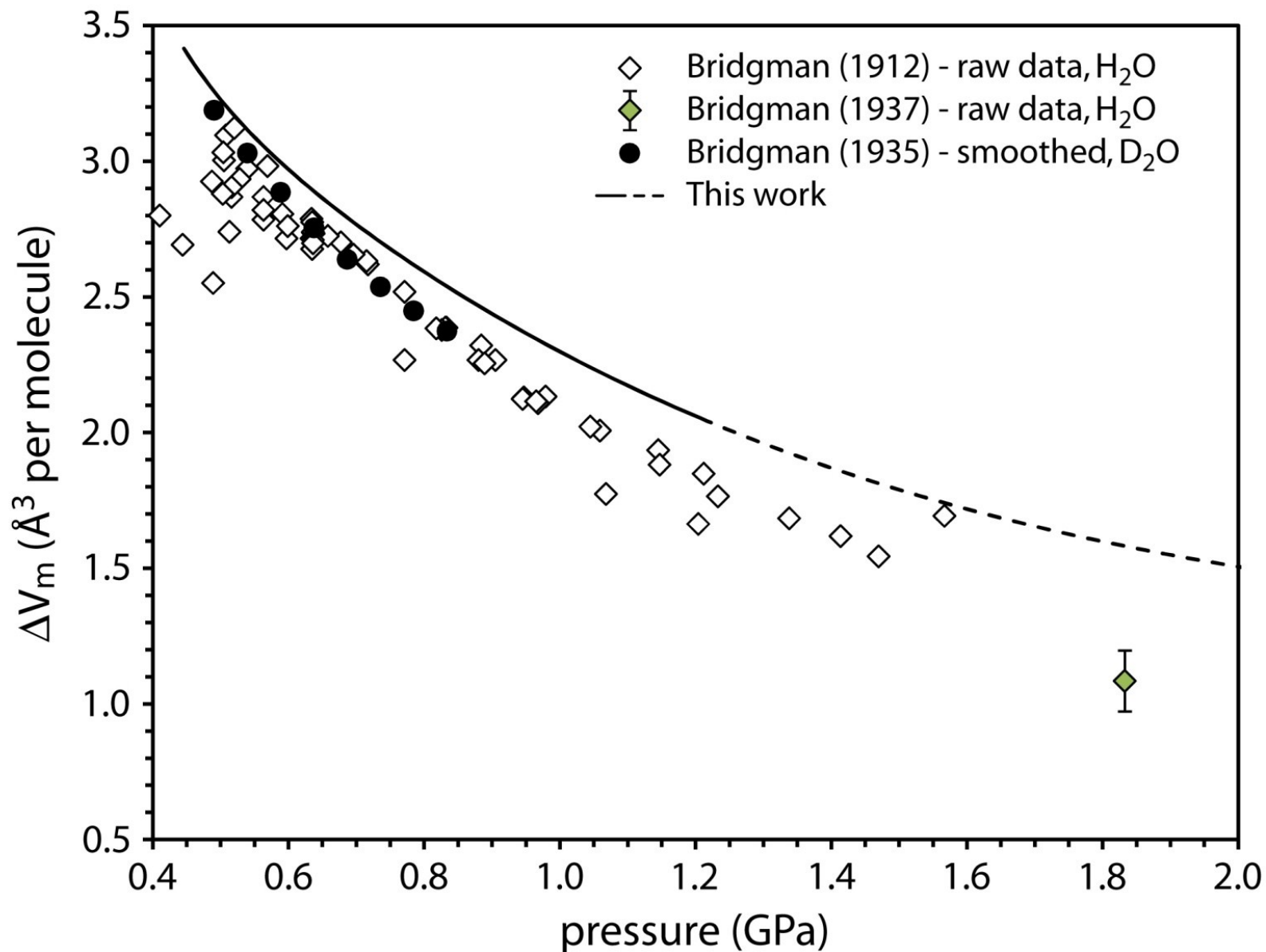
Measurements made en-route to ice-VI



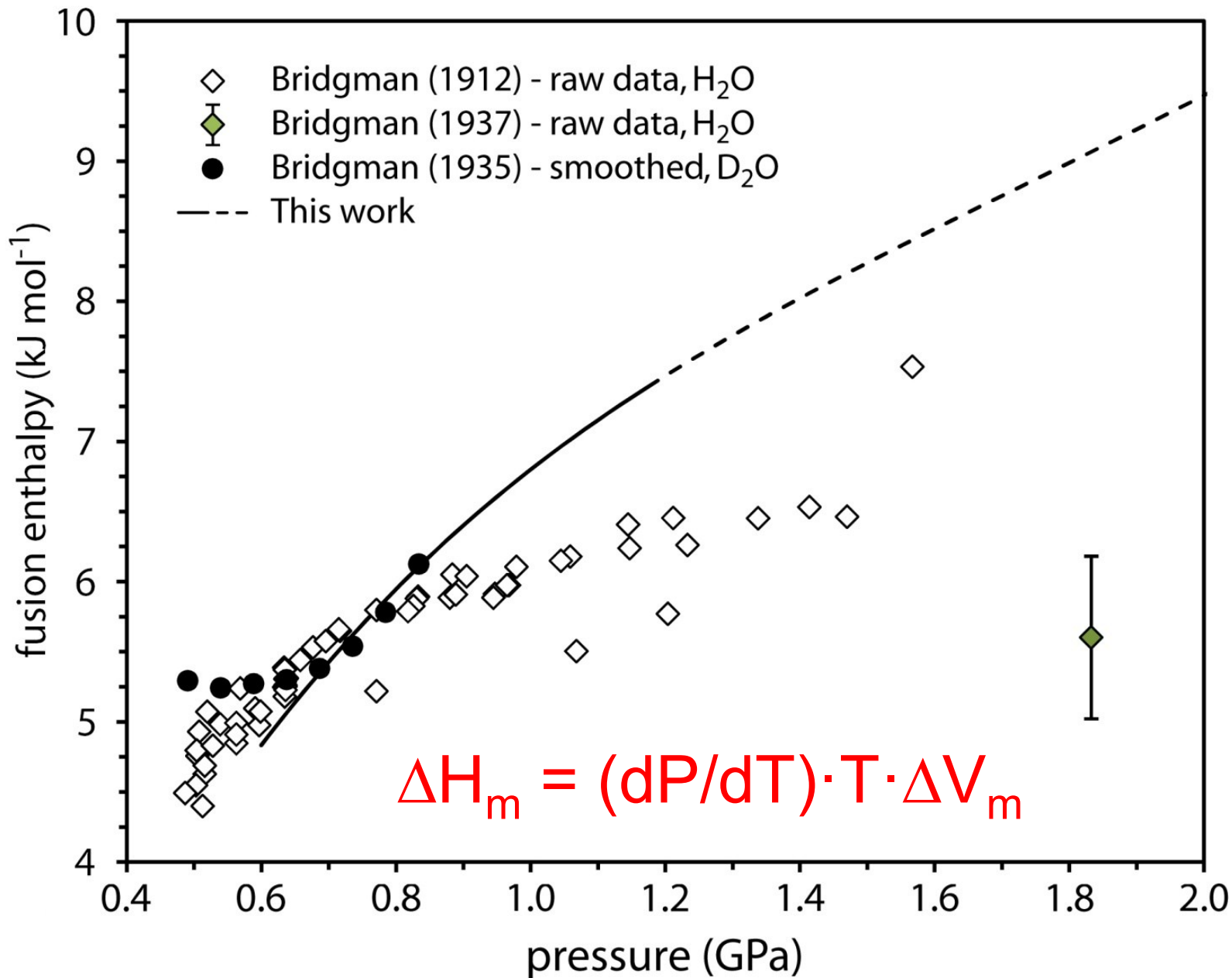
Pressure-Volume-Temperature (PVT) surface for ice-VI



Volume of fusion, ΔV_m calculated from the new equation of state

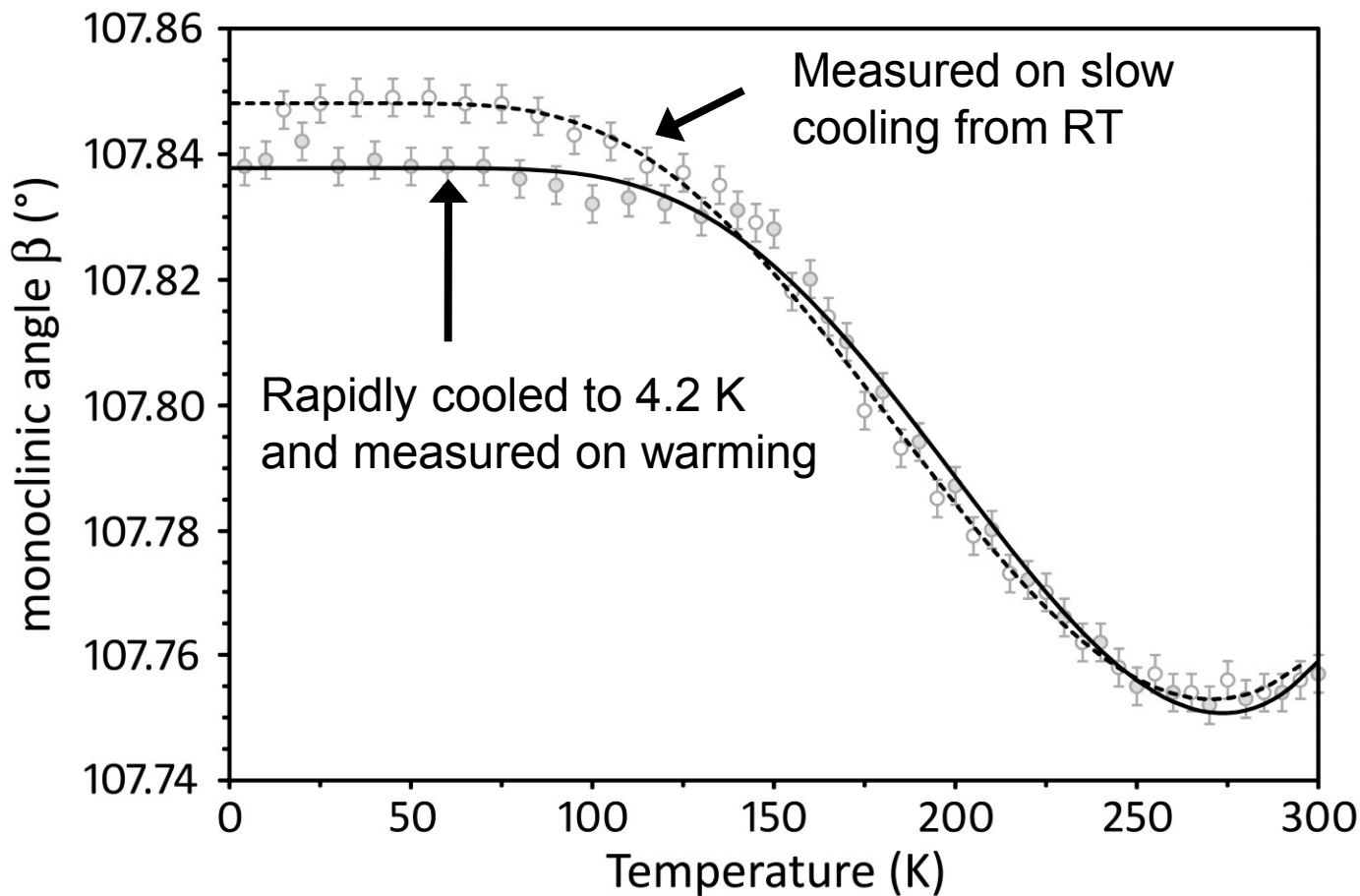


Enthalpy of fusion, ΔH_m calculated from the new equation of state

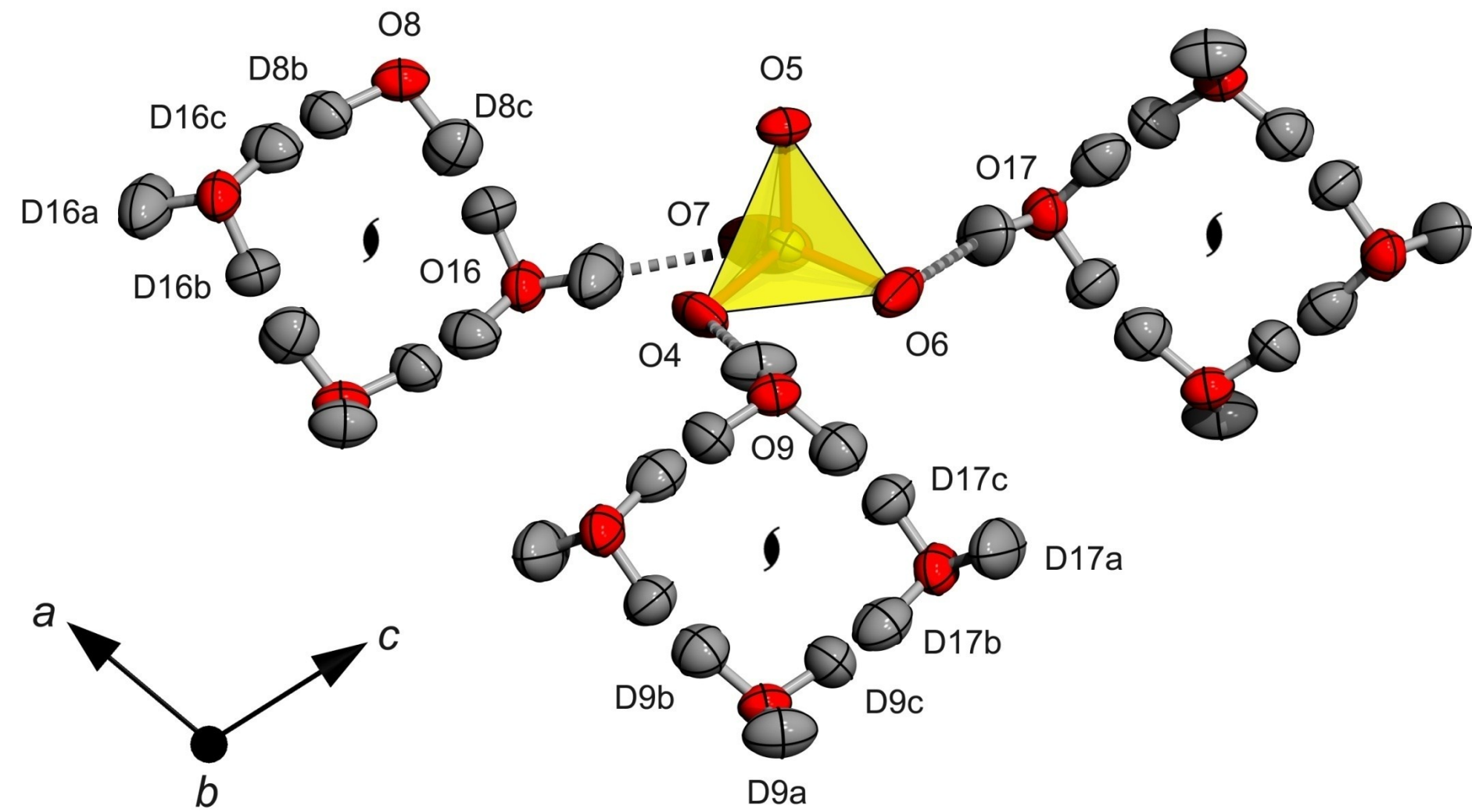


Case study 4:

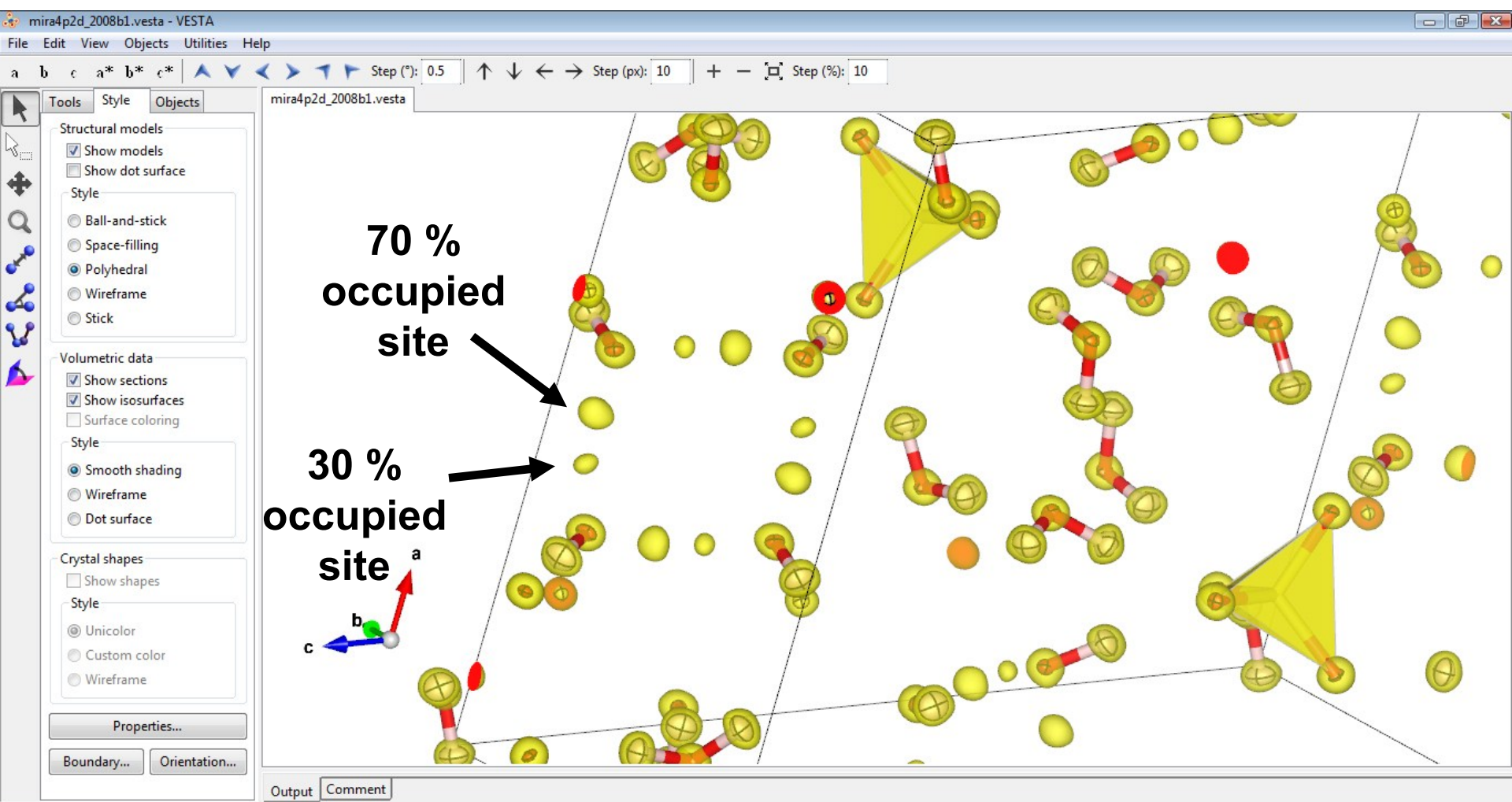
Understanding the thermal expansion of mirabilite from single-crystal data



The mirabilite structure contains two symmetry independent rings of orientationally disordered water molecules. At room T, the hydrogen atom sites in the rings are apparently half-occupied.



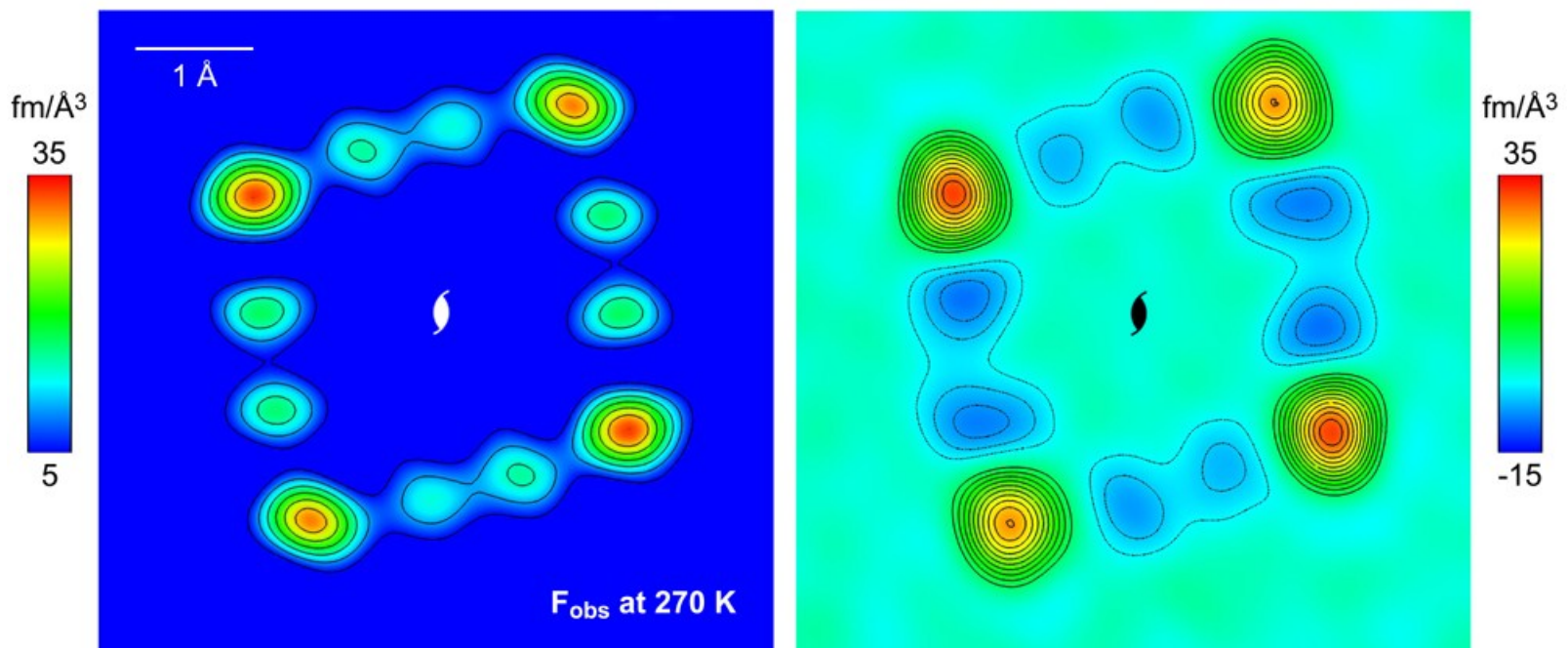
VESTA is a useful tool for visualising scattering density maps



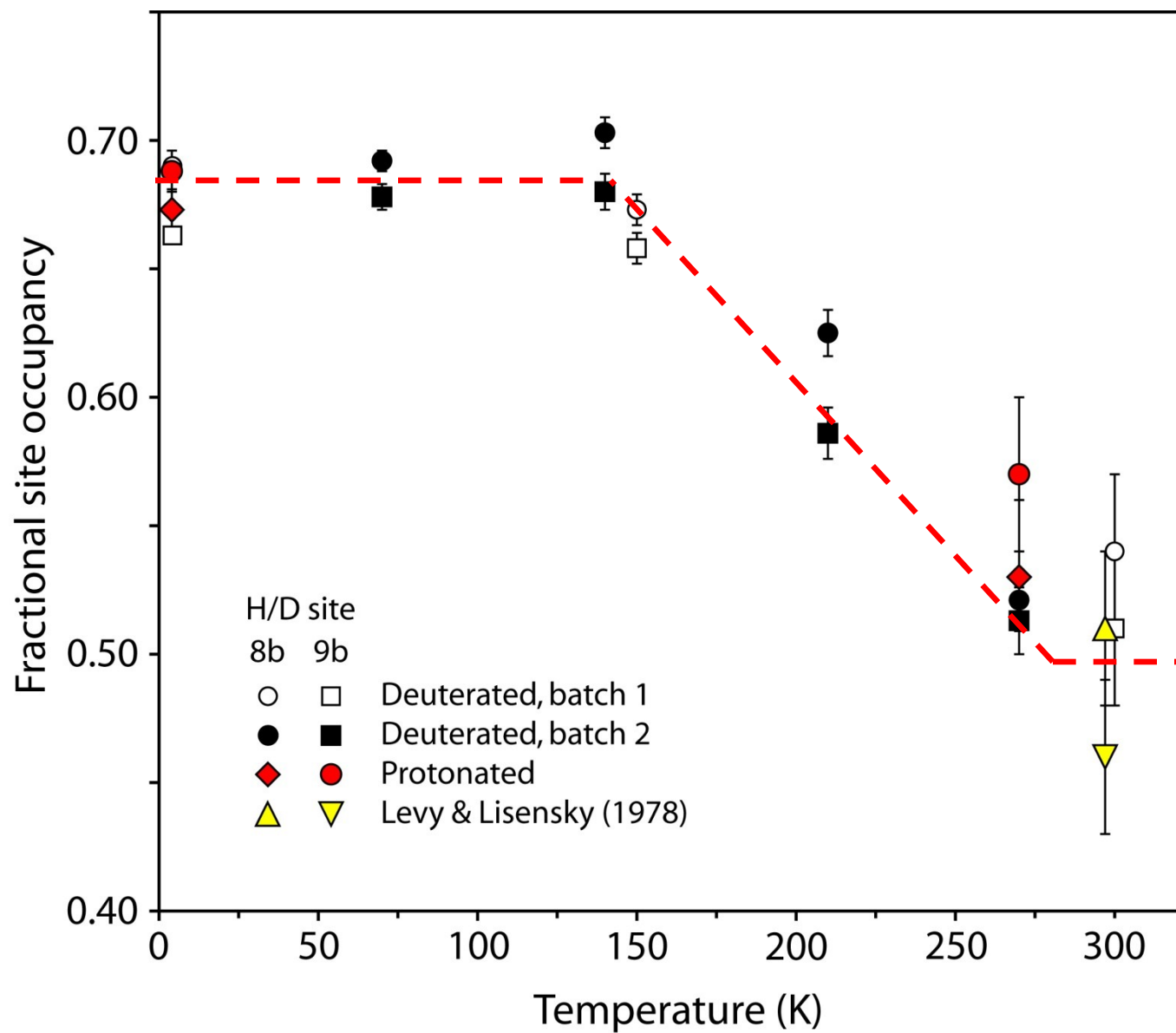
Results

Twenty degrees below room T, we find that the hydrogen atoms sites in the square rings are completely disordered (50 % occupancy) in both ordinary and heavy mirabilite

Note that deuterons produce positive peaks in the F_{obs} maps whereas protons (with a negative scattering length) produce holes, or negative peaks.



Variation in site occupancies as a function of temperature from SXD data



Thanks to all the colleagues
who have made this work
possible, including

Ian Wood, Matt Tucker, Bill
Marshall, Kevin Knight, and the
many ISIS Technical & Support
staff.

Thanks also to the STFC ISIS
Neutron Source for the beam-
time required to carry out these
measurements.



Thankyou!